Residual Transceiver Hardware Impairments on Cooperative NOMA Networks

Xingwang Li, *Member, IEEE,* Jingjing Li, *Student Member, IEEE,* Yuanwei Liu, *Member, IEEE,*
Zhiguo Ding, *Senior Member, IEEE,* and Arumugam Nallanathan, *Fellow, IEEE*

Abstract—This paper investigates the impact of residual transceiver hardware impairments (RTHIs) on cooperative non-orthogonal multiple access (NOMA) networks, where generic $\alpha - \mu$ fading channel is considered. To be practical, imperfect channel state information (CSI) and imperfect successive interference cancellation (SIC) are taken into account. More particularly, two representative NOMA scenarios are proposed, namely non-cooperative NOMA and cooperative NOMA. For the non-cooperative NOMA, the base station (BS) directly performs NOMA with all users. For the cooperative NOMA, the BS communicates with NOMA users with the aid of an amplify-and-forward (AF) relay, and the direct links between BS and users are existent. To characterize the performance of the proposed networks, new closed-form and asymptotic expressions for the outage probability (OP), ergodic capacity (EC) and energy efficiency (EE) are derived, respectively. Specifically, we also design the relay location optimization algorithms from the perspectives of minimize the asymptotic OP. For non-cooperative NOMA, it is proved that the OP at high signal-to-noise ratios (SNRs) is a function of threshold, distortion noises, estimation errors and fading parameters, which results in 0 diversity order. In addition, *high SNR slopes* and *high SNR power offsets* achieved by users are studied. It is shown that there are rate ceilings for the EC at high SNRs due to estimation error and distortion noise, which cause 0 *high SNR slopes* and ∞ *high SNR power offsets*. For cooperative NOMA, similar results can be obtained, and it also demonstrates that the outage performance of cooperative NOMA scenario exceeds the non-cooperative NOMA scenario in the high SNR regime.

Index Terms—$\alpha-\mu$ fading channels, hardware impairments, imperfect CSI, imperfect SIC, NOMA

I. INTRODUCTION

WITH unprecedented application of smart devices, wireless communications operators are facing a great challenge due to the exponentially increasing data service [2]. Non-orthogonal multiple access (NOMA) has been proposed as a promising technique to address this challenge for the fifth-generation (5G) mobile networks, such as spectrum efficiency, quality-of-service (QoS) and massive connectivity [3]. In general, NOMA techniques can be classified into two categories, namely, code-domain NOMA [4] and power-domain NOMA

[5].[1] The dominant feature of NOMA is to allow multiple users to share the same time/frequency/code resources with different power allocation according to their channel conditions. At the receiver, the superimposed information is decoded by using successive interference cancelation (SIC) algorithms [6].

Recently, NOMA has been extensively studied in wireless communication [7–10], and some of NOMA techniques have been accepted by 3GPP, e.g. downlink multiuser superposition transmission [11] and massive machine type communication [12]. In [7], the performance of downlink NOMA systems was studied for randomly deployed users, in which analytical expressions for the outage probability (OP) were derived in closed-form. [8] proposed a new power control scheme and derived closed-form expressions for the OP and achievable sum rate of uplink NOMA systems. With the emphasis on physical layer security, [9] investigated the secrecy performance of large-scale NOMA networks, where both single-antenna and multiple-antenna assisted transmission scenarios were considered. The coverage, ergodic capacity (EC) and energy efficiency (EE) of large-scale heterogeneous networks (HetNets) were analyzed in [13], where a new transmission framework combining NOMA with HetNets was proposed. Considering the combination of NOMA and simultaneous wireless information and power transfer (SWIPT) technologies, a cooperative SWIPT NOMA protocol was proposed in [10], where users with better channel conditions were used as energy harvesting relays to help users with worse channel conditions.

One common characteristic of the aforementioned works is that perfect radio frequency (RF) components are assumed at the transceivers, which is impractical for the realistic systems. In practice, all RF components suffer from several types of hardware impairments, such as amplifier non-linearities, in-phase/quadrature imbalance, phase noise, quantization error [14]. Although some compensation and calibration algorithms are used to mitigate the influence of such individual hardware impairments, there are still some residual transceiver hardware impairments (RTHIs) due to estimation error, inaccurate calibration and different types of noise [15]. Theoretic analysis and experiment results have demonstrated that the RTHIs can be modelled by an additive distortion noise [14, 16]. To this end, several works have studied the aggregated impact of RTHIs on system performance [17–19]. [17] indicated that RTHIs resulted in a fundamental capacity ceiling, which can

---

[1]In this paper, we focuses on power-domain NOMA techniques, and we simply use "NOMA" to refer to "power-domain NOMA".

not be eliminated by increasing the transmit power. In [18], authors proposed a linear channel estimator in the presence of RTHIs. Considering two types of relay selection strategies, the outage behavior of decode-and-forward (DF) relaying networks in the presence of RTHIs and co-channel interference was explored in [19].

A. Motivation and Related Works

Although the aforementioned works have laid a solid foundation with providing a good understanding of NOMA and RTHIs, to the best of our knowledge, the only relevant studies have been reported in [20–22] and [23–25]. In [20], authors investigated the performance of NOMA-based cooperative full/half-duplex relaying networks and derived closed-form expressions for the exact OP and the network throughput. Regarding the line-of-sight propagation environments, an approximate analysis method for NOMA-based relaying systems over Rician fading channels was proposed in [21]. Authors in [22] analyzed the outage behavior of amplify-and-forward (AF) NOMA relaying and derived closed-form expressions for the exact OP and lower/upper bounds. As for hardware impairments, [23] quantified the impact of residual hardware impairments on AF and DF relaying networks over Rayleigh and Nakagami-m fading channels. In [24], the exact expressions for the OP and symbol error rates of two-way AF relaying networks were derived, where hardware impairments at the relay node is considered. The outage performance of SWIPT cooperative multi-relay networks with hardware impairments constraints have been investigated in [25].

More recently, [26] has analyzed the impact of RTHIs on the performance of NOMA-based AF relaying network under the assumption of no direct link. Nonetheless, it has the assumption that perfect channel state information (CSI) is available, which is a great challenge due to estimation errors and feedback delay. Cooperative NOMA relay systems with CSI for ideal hardware conditions were studied in [27, 28]. [27] investigated the performance for the relay-aided NOMA systems under the condition of statistical CSI. [28] studied the performance of NOMA by assuming two types of imperfect CSI, namely estimation error and statistics CSI. Also, the joint impact of RTHIs and imperfect CSI has been studied in [29], but not in cooperative NOMA networks. Moreover [29] analyzed the joint impact of RTHIs and imperfect CSI on the outage performance of multiple antenna systems with SIC detections. In practical systems, the decoding error might be inevitable during SIC detections, which results that the interference cannot be canceled completely, namely imperfect SIC [30]. Therefore, there is still a dearth of research contributions on the performance analysis of cooperative NOMA networks with RTHIs, imperfect CSI and imperfect SIC.

B. Contributions

Motivated by the aforementioned discussion, in this paper, we study the impact of RTHIs and imperfect SIC on cooperative NOMA relaying networks. In addition, imperfect CSI is taken into account by considering two representative channel estimation models: *i)* The variance of channel estimation

error is a non-negative fixed constant; *ii)* The variance of the channel estimation error is a function of the transmit average SNR. The generic $\alpha-\mu$ fading channel is adopted since it is widely used to characterize the nature of non-homogeneous fading environment, where the surfaces are correlated nonlinear environment [31]. In addition, based on the different parameter settings, this versatile model can be used to capture the fading characteristics of several channels. For instance, Gamma (α=1), Nakagami-m (α=2, μ= m), Weibull ($\alpha = m, \mu = 1$), and Rayleigh ($\alpha = 2, \mu = 1$) [31]. Unfortunately, a $\alpha - \mu$ model makes the analysis of cooperative NOMA networks more complicated, as the results of the above fading model cannot be directly extended to this one. Moreover, two typical scenarios are considered: *i)* The base station (BS) directly sends information to multiple users, namely non-cooperative NOMA; *ii)* The BS communicates with users with the assistance of an AF relay, and the direct links between BS and users are existent, namely cooperative NOMA.

Different from [32]: *i)* We investigate the effect of RTHIs and imperfect CSI on the system OP, EC and EE; *ii)* We consider the more realistic case, where the imperfect SIC exists during the procedure of SIC; *iii)* Relay location optimization for the cooperative NOMA scenario is analyzed.

The primary contributions of this paper are summarized as:

- *Non-cooperative NOMA:* We derive exact expressions for the OP of the near user and the far user. To obtain more insights, we further carry out the asymptotic analysis in terms of OP at high signal-to-noise ratios (SNRs) for the two users and obtain diversity orders. We demonstrate that for the first estimation model, the diversity order is zero, while for the second estimation model, the diversity order is fixed constant, which is determined by fading parameter and the number of users.

- *Non-cooperative NOMA:* We derive the analytical expression in terms of EC for the two users. For obtaining more insights, we further derive the *high-SNR slopes* and *high-SNR power offsets* for the EC in the high SNR region. It reveals that there exist capacity ceilings in the presence of distortion noise and channel estimation error, which results in zero *high-SNR slopes* and infinity *high-SNR power offsets*.

- *Cooperative NOMA:* We derive the closed-form expressions for the OP of cooperative NOMA. To obtain deeper insights, the asymptotic behaviors and diversity orders are explored in the high SNR regime. Similarly, we demonstrate that for the first estimation model, there are error floors for the OP, which results in zero diversity orders. For the second estimation model, the OP can be improved as the SNR increasing and diversity order approaches a positive constant.

- *Cooperative NOMA:* We study the ergodic capacities by deriving approximate closed-form expressions for the two users. Similarly, the *high-SNR slope* and *high-SNR power offset* analyses are carried out. The results clearly show that there are rate ceilings for the EC, which results in 0 *high-SNR slopes* and ∞ *high-SNR power offsets*. For ideal conditions, *high-SNR slope* is $1/2$, and *high-SNR*
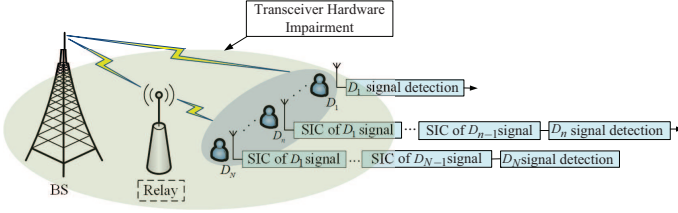
Fig. 1: Illustration of multiuser NOMA networks

power offset is constant, which is determined by fading parameters and the number of users.

- *Relay Location Optimization:* For the cooperative NOMA, we optimize the relay location with fixed power allocation from the perspectives of minimize the asymptotic OP of the considered networks.
- *Energy efficiency:* We analyze the EE performance of the considered communication networks. We conclude that estimation errors have significant effects on the system EE at mid SNRs. Additionally, by optimizing the relay location, cooperative NOMA has a higher EE corresponding to non-cooperative NOMA since cooperative NOMA scheme can achieve higher EC than that of non-cooperative NOMA.

C. Organization and Notations

The remainder of this paper is organised as follows. In Section II, we introduce the general hardware impairment model for the two scenarios. In Section III, new analytical expressions for the OP and diversity order are derived and discussed. In Section IV, approximate analytical expressions for the EC are derived and the asymptotic analyses in terms of *high SNR slope* and *high SNR power offset* are analyzed. The location optimization problem is formulated and analyzed in Section V. Section VI evaluates the EE of overall networks. Section VII showcases numerical results according to the Monte-Carlo simulations to validate the correctness of theoretical analyses. Section VIII concludes the paper and summarize the key findings.

We use $\mathbb{E}\{\cdot\}$ to denote the expectation operation, while $\triangleq$ denotes definition operation. A complex Gaussian random variable with mean μ and variance σ^2 reads as $\mathcal{CN}\{\mu, \sigma^2\}$. $\Gamma\{\cdot\}$ represents the Gamma function, while $n!$ is the factorial operation. Finally, $f_X(\cdot)$ and $F_X(\cdot)$ are the probability density function (PDF) and the cumulative distribution function (CDF) of a random variable, respectively.

II. SYSTEM MODEL

We consider a cooperative NOMA AF relay network as depicted in Fig. 1. There is one source (S), i.e, BS, that aims to communicate with N destinations (D) with the aid of an AF relay (R). In this paper, two typical scenarios are considered: *i)* S directly communicates with D_n $(1 \leq n \leq N)$; *ii)* S communicates with users D_n with the help of an AF relay R, and the direct links between S and D_n are existent. We assume all nodes are equipped with one antenna. We also assume that d_{sr} is the distance between S and R, d_{sd_n} is the

distance between S and D_n, d_{rd_n} is the distance between R and D_n.

In practice, perfect CSI is supposed to be unavailable due to some types of errors. The common way to obtain CSI is channel estimation[2]. By using linear minimum mean square error (LMMSE), the channel coefficient is denoted by

$$g_i = \hat{g}_i + e_i \, (i = sr, rd_n, sd_n) \tag{1}$$

where $\hat{g}_i$ denotes the estimated channel coefficient, and $e_i \sim \mathcal{CN}\left(0, \sigma_{e_i}^2\right)$ represents the channel estimation error. Note that $\hat{g}_i$ and e_i are uncorrelated due to the orthogonality property of LMMSE algorithm.

In this paper, we consider two types of channel estimation error models:

1) $\sigma_{e_i}^2$ is fixed and independent of the average SNR;

2) $\sigma_{e_i}^2$ is a function of the average SNR, where $\sigma_{e_i}^2$ can be approximated as a Gaussian random variable [33]. The variance of the error can be modeled as $\sigma_{e_i}^2 = \Omega_i/(1 + \delta\gamma\Omega_i)$, where $\Omega_i = d_i^{-\tilde{\alpha}}$ is the variance of g_i, γ is the transmit SNR, $\delta > 0$ depends on the cost of acquiring CSI in the light of the training pilots power consumption and reflects the quality of channel estimation. It is worth pointing out that δ can be expressed as $\delta = \varepsilon L$ [34], where ε denotes the ratio of pilot energy to date energy, L denotes the number of pilot symbols. Thus, the variance of the estimated channel $\hat{g}_i$ can be given as $\hat{\Omega}_i = \Omega_i - \sigma_{e_i}^2 = \delta\gamma\Omega_i^2/(1 + \delta\gamma\Omega_i)$.

Defining channel gain $\rho_i = |\hat{g}_i|^2$, as in [35], the PDF and CDF of estimated channel are given as.

$$f_{\rho_i}(x) = \frac{\alpha_i x^{\frac{\alpha_i \mu_i}{2} - 1}}{2\beta_i^{\frac{\alpha_i \mu_i}{2}} \Gamma(\mu_i)} e^{-\left(\frac{x}{\beta_i}\right)^{\frac{\alpha_i}{2}}}, i = sr, rd_n, sd_n, \tag{2}$$

$$F_{\rho_i}(x) = 1 - \sum_{m=0}^{\mu_i-1} \frac{e^{-\left(\frac{x}{\beta_i}\right)^{\frac{\alpha_i}{2}}}}{m!} \left(\frac{x}{\beta_i}\right)^{\frac{\alpha_i m}{2}}, \tag{3}$$

where $\alpha_i > 0$ and $\mu_i > 0$ are the nonlinearity power exponent and the number of multipath cluster, respectively, $\beta_i \triangleq \mathbb{E}(x)\Gamma(\mu_i)/\Gamma(\mu_i + 2/\alpha_i)$, $\mathbb{E}(x) = \hat{r}_i^2\Gamma(\mu_i + 2/\alpha)/(\mu_i^{2/\alpha_i}\Gamma(\mu_i))$, where $\hat{r}_i$ is defined as the $\hat{r}_i = \sqrt[\alpha_i]{\mathbb{E}(R^{\alpha_i})}$-root mean of the amplitude of random variable.

Using order statistics [36], the PDF and CDF of the ordered variable, $\tilde{\rho}_{sd_n}$, are given by

$$f_{\tilde{\rho}_{sd_n}}(x) = \Xi \sum_{k=0}^{N-n} (-1)^k \binom{N-n}{k} f_{\rho_{sd_n}}(x) \left[F_{\rho_{sd_n}}(x)\right]^{n+k-1}, \tag{4}$$

$$F_{\tilde{\rho}_{sd_n}}(x) = \Xi \sum_{k=0}^{N-n} \binom{N-n}{k} \frac{(-1)^k}{n+k} \left[F_{\rho_{sd_n}}(x)\right]^{n+k}, \tag{5}$$

where $\Xi = \frac{N!}{(n-1)!(N-n)!}$.

Without loss of generality, we assumed that the estimated channel gain between S and D_n are sorted as $|\hat{g}_{sd_1}|^2 \leq |\hat{g}_{sd_1}|^2 \leq \cdots \leq |\hat{g}_{sd_N}|^2$ [5].

---

[2]In practice, in order to obtain the knowledge of the channel, the transmitter is requires to send training sequence to receiver during some portion of the transmission interval.

A. Non-cooperative NOMA

According to NOMA protocol, S sends $\sum_{n=1}^{N} \sqrt{a_n P_s} x_n$ to D_n, where x_n is the message for the n-th user with $\mathbb{E}(|x_n|^2) = 1$, P_s is the average transmit power of S, a_n is the power allocation coefficient for ensuring the fairness among users with $a_1 > a_2 > \cdots > a_N$, and $\sum_{n=1}^{N} a_n = 1$. Thus, referring to channel estimation error mode in [37] and distortion noise model in [23], the received signal at D_n is expressed as

$$y_{sd_n} = (\hat{g}_{sd_n} + e_{sd_n}) \left(\sum_{n=1}^{N} \sqrt{a_n P_s} x_n + \eta_{sd_n} \right) + n_{sd_n}, \quad (6)$$

where $\eta_{sd_n} \sim \mathcal{CN}\left(0, \kappa_{sd_n}^2 P_s\right)$ is the aggregated distortion noise from transceiver; κ_{sd_n} represents the level of hardware impairment at transceivers, which can be measured in practice based on the error vector magnitude (EVM) [38]; $n_{sd_n} \sim \mathcal{CN}\left(0, N_{sd_n}\right)$ represents the additive white complex Gaussian noise (AWGN). In addition, we define $\gamma = P_s / N_{sd_n}$.

According to NOMA protocol, SIC is carried out at users. Considering imperfect SIC, the received signal-to-interference-plus-noise ratio (SINR) for D_n to decode D_j's message x_j, $j \leq n$, can be expressed as

$$\gamma_{sd,j\to n} = \frac{a_j \gamma \tilde{\rho}_{sd_n}}{\gamma \left(\tilde{\Delta}_j + \Delta_j + \kappa_{sd_n}^2 \right) \tilde{\rho}_{sd_n} + d_{sd_n}^{\tilde{\alpha}} \left(\sigma_{e_{sd_n}}^2 \gamma \left(1 + \kappa_{sd_n}^2\right) + 1 \right)}, \quad (7)$$

where $\tilde{\Delta}_j = \sum_{\tilde{p}=1}^{j-1} \xi_{\tilde{p}} a_{\tilde{p}}$, $0 < \xi_{\tilde{p}} < 1$ indicates imperfect SIC, $\xi_{\tilde{p}} = 0$ and $\xi_{\tilde{p}} = 1$ denote perfect SIC and no SIC, respectively; $\Delta_j = \sum_{p=j+1}^{N} a_p$, $\tilde{\alpha}$ is the path loss parameter. If x_j is detected under the condition of imperfect SIC, the received SINR at D_n to detect its own message is given by

$$\gamma_{sd_n} = \frac{a_n \gamma \tilde{\rho}_{sd_n}}{\gamma \left(\tilde{\Delta}_n + \Delta_n + \kappa_{sd_n}^2 \right) \tilde{\rho}_{sd_n} + d_{sd_n}^{\tilde{\alpha}} \left(\sigma_{e_{sd_n}}^2 \gamma \left(1 + \kappa_{sd_n}^2\right) + 1 \right)}, \quad (8)$$

where $\tilde{\Delta}_n = \sum_{\tilde{p}=1}^{n-1} \xi_{\tilde{p}} a_{\tilde{p}}$, $\Delta_n = \sum_{q=n+1}^{N} a_q$.

B. Cooperative NOMA

For cooperative NOMA, the entire transmission process is accomplished in two time slots.

The first phase: S transmits the superposed signal to R and D_n according to the NOMA protocol. Thus, the received signal at R and D_n are given as

$$y_{\tilde{i}} = (\hat{g}_{\tilde{i}} + e_{\tilde{i}}) \left(\sum_{n=1}^{N} \sqrt{a_n P_s} x_n + \eta_{\tilde{i}} \right) + n_{\tilde{i}}, \tilde{i} = sr, sd_n, \quad (9)$$

where $\eta_{\tilde{i}} \sim \mathcal{CN}\left(0, \kappa_{\tilde{i}}^2 P_s\right)$ denote the distortion noise from transceivers, $n_{\tilde{i}} \sim \mathcal{CN}\left(0, N_{\tilde{i}}\right)$ is the AWGN noise.

At the receivers, the received SINR at D_n to decode D_j's message x_j, $j \leq n$ under imperfect SIC, is expressed as

$$\gamma_{sd,j\to n} = \frac{a_j \gamma \tilde{\rho}_{sd_n}}{\gamma \left(\tilde{\Delta}_j + \Delta_j + \kappa_{sd_n}^2 \right) \tilde{\rho}_{sd_n} + d_{sd_n}^{\tilde{\alpha}} \left(\sigma_{e_{sd_n}}^2 \gamma \left(1 + \kappa_{sd_n}^2\right) + 1 \right)}, \quad (10)$$

For the case of imperfect SIC, after D_j's message x_j is detected, the received SINR at D_n to detect its own message x_n is given by

$$\gamma_{sd_n} = \frac{a_n \gamma \tilde{\rho}_{sd_n}}{\gamma \left(\tilde{\Delta}_n + \Delta_n + \kappa_{sd_n}^2 \right) \tilde{\rho}_{sd_n} + d_{sd_n}^{\tilde{\alpha}} \left(\sigma_{e_{sd_n}}^2 \gamma \left(1 + \kappa_{sd_n}^2\right) + 1 \right)}, \quad (11)$$

The second phase: The relay amplifies and forwards the received signal to the intended users, then the received signal at D_n is obtained as

$$y_{rd_n} = (\hat{g}_{rd_n} + e_{rd_n}) (G y_{sr} + \eta_{rd_n}) + n_{rd_n}, \quad (12)$$

where $G \triangleq \sqrt{\frac{P_r}{P_s(1+\kappa_{sr}^2)|\hat{g}_{sr}|^2 + P_s(1+\kappa_{sr}^2)\sigma_{e_{sr}}^2 + N_{sr}}}$ is the amplification factor, $\eta_{rd_n} \sim \mathcal{CN}\left(0, \kappa_{rd_n}^2 P_r\right)$ is the aggregated distortion noise from R and D_n, $n_{rd_n} \sim \mathcal{CN}\left(0, N_{rd_n}\right)$ represents AWGN noise, P_r is the transmit power at R. For convenience, we have the following definitions: $\lambda_{sr} = P_s/N_{sr}$ and $\lambda_{rd_n} = P_r/N_{rd_n}$ as the SNR at S and R, respectively. We further assume $\lambda_{sr} = c_1 \gamma$, $\lambda_{rd_n} = c_2 \gamma$, where c_1 and c_2 are constants.

Here, the SIC can be invoked by D_n for detecting D_j. Thus, the SINR for D_n to decode D_j's message under the condition of imperfect SIC can be given by

$$\gamma_{rd,j\to n} = \frac{a_j c_1 c_2 \gamma^2 \rho_{sr} \rho_{rd_n}}{c_1 c_2 a_j \gamma^2 \left(\tilde{\Delta}_j + \Delta_j + d \right) \rho_{sr} \rho_{rd_n} + \phi_{1,n} c_1 \gamma \rho_{sr} + \phi_{2,n} c_2 \gamma \rho_{rd_n} + \phi_{3,n}}, \quad (13)$$

where $d = \kappa_{sr}^2 + \kappa_{rd_n}^2 + \kappa_{sr}^2 \kappa_{rd_n}^2$, $\phi_{1,n} = d_{rd_n}^{\tilde{\alpha}} \left(c_2 \gamma \sigma_{e_{rd_n}}^2 (1+d) + \kappa_{sr}^2 + 1 \right)$, $\phi_{2,n} = d_{sr}^{\tilde{\alpha}} \left(c_1 \gamma \sigma_{e_{sr}}^2 (1+d) + \kappa_{rd_n}^2 + 1 \right)$, $\phi_{3,n} = d_{sr}^{\tilde{\alpha}} d_{rd_n}^{\tilde{\alpha}} \times \left(c_1 c_2 \gamma^2 \sigma_{e_{sr}}^2 \sigma_{e_{rd_n}}^2 (1+d) + c_1 \gamma \sigma_{e_{sr}}^2 (1+\kappa_{sr}^2) + c_2 \gamma \sigma_{e_{rd_n}}^2 (1+\kappa_{rd_n}^2) + 1 \right)$.

Considering imperfect SIC, when the message x_j is decoded from the superposed message, the SINR for D_n to decode its own message is obtained as

$$\gamma_{rd_n} = \frac{a_n c_1 c_2 \gamma^2 \rho_{sr} \rho_{rd_n}}{c_1 c_2 \gamma^2 \left(\tilde{\Delta}_n + \Delta_n + d \right) \rho_{sr} \rho_{rd_n} + \phi_{1,n} c_1 \gamma \rho_{sr} + \phi_{2,n} c_2 \gamma \rho_{rd_n} + \phi_{3,n}}. \quad (14)$$

III. OUTAGE PROBABILITY ANALYSIS

In this section, we explore the outage behaviors for the two scenarios by deriving the exact expressions for the OP.

A. Non-cooperative NOMA

1) OP: The outage event occurs at D_n when D_n fails to decode its own signal or the signal of D_j, the OP at D_n can be expressed as

$$P_{out}^n = 1 - \Pr\left(E_{n,1}^{sd} \cap \cdots \cap E_{n,n}^{sd} \right), \quad (15)$$

where $E_{n,j}^{sd}$ denotes D_n can successfully decode D_j's signal, which can be expressed as

$$
\begin{aligned}
E_{n,j}^{sd} &= \{\gamma_{sd,j\to n} > \gamma_{thj}\} \\
&= \left\{ \tilde{\rho}_{sd_n} > \frac{\gamma_{thj} d_{sd_n}^{\tilde{\alpha}} \left(\sigma_{e_{sd_n}}^2 \gamma \left(1 + \kappa_{sd_n}^2\right) + 1 \right)}{\gamma \left(a_j - \left(\tilde{\Delta}_j + \Delta_j + \kappa_{sd_n}^2 \right) \gamma_{thj} \right)} \triangleq \theta_j \right\},
\end{aligned} \quad (16)
$$

where γ_{thj} is the target date of D_j, (16) satisfies $a_j > \left(\tilde{\Delta}_j + \Delta_j + \kappa_{sd_n}^2\right)\gamma_{thj}$.

The exact expressions for the OP of D_n for ideal/non-ideal conditions are given in the following theorem. All through this paper, we have $\kappa_{sr} = \kappa_{rd_n} = \kappa_{sd_n} \neq 0, \sigma_{e_s r} = \sigma_{e_{rd_n}} = \sigma_{e_{sd_n}} \neq 0, \xi_{\tilde{p}} \neq 0$ and $\kappa_{sr} = \kappa_{rd_n} = \kappa_{sd_n} = 0, \sigma_{e_s r} = \sigma_{e_{rd_n}} = \sigma_{e_{sd_n}} = 0, \xi_{\tilde{p}} = 0$ for non-ideal conditions and ideal conditions, respectively.

Theorem 1. *For $\alpha - \mu$ fading channels, the exact analytical expressions for the OP of D_n can be given as*[3]
  * *Non-ideal conditions*

$$P_{out}^{n,\mathrm{ni}} = \Xi \sum_{k=0}^{N-n} \binom{N-n}{k} \frac{(-1)^k}{n+k} \left(1 - \sum_{m_1=0}^{\mu_{sd_n}-1} \frac{e^{-\left(\frac{\theta_n^*}{\beta_{sd_n}}\right)^{\frac{\alpha_{sd_n}}{2}}} \left(\frac{\theta_n^*}{\beta_{sd_n}}\right)^{\frac{\alpha_{sd_n} m_1}{2}}}{m_1!}\right)^{n+k},$$
(17)

where $\theta_n^* = \max\limits_{1\leq j\leq n} \theta_j$.
  * *Ideal conditions*

$$P_{out}^{n,\mathrm{id}} = \Xi \sum_{k=0}^{N-n} \binom{N-n}{k} \frac{(-1)^k}{n+k} \left(1 - \sum_{m_1=0}^{\mu_{sd_n}-1} \frac{e^{-\left(\frac{\vartheta_1}{\beta_{sd_n}}\right)^{\frac{\alpha_{sd_n}}{2}}} \left(\frac{\vartheta_1}{\beta_{sd_n}}\right)^{\frac{\alpha_{sd_n} m_1}{2}}}{m_1!}\right)^{n+k}.$$
(18)

where $\vartheta_1 = \max\limits_{1\leq j\leq n} \frac{\gamma_{thj} d_{sd_n}^{\tilde{\alpha}}}{\gamma(a_j - \Delta_j \gamma_{thj})}$.

Proof: By plugging (16) into (15), we can obtain

$$P_{out}^n = 1 - \Pr\left\{\tilde{\rho}_{sd_n} > \theta_n^*\right\}.$$
(19)

where $\theta_n^* = \max\limits_{1\leq j\leq n} \theta_j$. Then, substituting (4) into (19), (17) can be obtained after some manipulations. For ideal conditions, the closed-form expression for the OP of users can be obtained by setting $\kappa_i = \sigma_{e_i}^2 = 0$. ∎

2) Diversity Order: In the presence of non-ergodic fading channels, diversity order is an key metric of performance evaluation, which can be used to characterize the effects of system and fading parameters on the OP of the proposed NOMA networks. To this end, we carry out the diversity order analysis in the high SNR region. Diversity order is defined as the negative slope of the OP versus SNR on the log-log scale as [39]

$$d = -\lim_{\gamma\to\infty} \frac{\log\left(P_{out}^{n,\infty}\right)}{\log\gamma}.$$
(20)

In the following, we first provide the asymptotic expression for the OP at high SNRs ($\gamma \to \infty$).

Corollary 1. *At high SNRs, the asymptotic OP for D_n can be given by*
  * *Non-ideal conditions*

$$P_{out,\infty}^{n,\mathrm{ni}} = \frac{\Xi'}{(\mu_{sd_n}!)^n} \left(\frac{\varsigma_1}{\beta_{sd_n}}\right)^{\frac{n\alpha_{sd_n}\mu_{sd_n}}{2}},$$
(21)

---

where $\varsigma_1 = \max\limits_{1\leq j\leq n} \frac{\gamma_{thj} d_{sd_n}^{\tilde{\alpha}} \sigma_{e_{sd_n}}^2 \left(1+\kappa_{sd_n}^2\right)}{a_j - \left(\tilde{\Delta}_j + \Delta_j + \kappa_{sd_n}^2\right)\gamma_{thj}}$. We note that $\varsigma_1 = \max\limits_{1\leq j\leq n} \frac{\gamma_{thj} d_{sd_n}^{\tilde{\alpha}} \left(1+\kappa_{sd_n}^2\right)}{\gamma\left(a_j - \left(\tilde{\Delta}_j + \Delta_j + \kappa_{sd_n}^2\right)\gamma_{thj}\right)}$ when $\sigma_{e_i}^2$ is a function of SNR.
  * *Ideal conditions*

$$P_{out,\infty}^{n,\mathrm{id}} = \frac{\Xi'}{(\mu_{sd_n}!)^n} \left(\frac{\vartheta_1}{\beta_{sd_n}}\right)^{\frac{n\alpha_{sd_n}\mu_{sd_n}}{2}}.$$
(22)

where $\vartheta_1 = \max\limits_{1\leq j\leq n} \frac{\gamma_{thj} d_{sd_n}^{\tilde{\alpha}}}{\gamma(a_j - \gamma_{thj}\Delta_j)}$, $\Xi' = \frac{N!}{n!(N-n)!}$.

Corollary 2. *The diversity orders of the n-th user for non-ideal/ideal conditions are given by*
  * *Non-ideal conditions: For fixed and variable estimation error model, the diversity order can be given respectively by*

$$d_{1st,f}^{n,\mathrm{ni}} = 0, \quad d_{1st,v}^{n,\mathrm{ni}} = \frac{n\alpha_{sd_n}\mu_{sd_n}}{2},$$
(23)
  * *Ideal conditions*

$$d_{1st}^{n,\mathrm{id}} = \frac{n\alpha_{sd_n}\mu_{sd_n}}{2}.$$
(24)

Proof: By plugging (22) into (20), the diversity order achieved by D_n is obtained. ∎

Remark 1. For ideal conditions, the OP is determined by the number of destinations and fading parameters. The diversity order is $\frac{n\alpha_{sd_n}\mu_{sd_n}}{2}$. For non-ideal conditions, when $\sigma_{e_i}^2$ is fixed, there is a floor for the OP, which is irrelated to the average SNR. For this case, diversity order is zero due to the fixed estimation error. When $\sigma_{e_i}^2$ is a function of SNR, the diversity order is the same with ideal conditions since the channel can be accurately estimated in the high SNR regime.

B. Cooperative NOMA

1) OP: In this scenario, the users can combine the received signals from the S and R by using selection combining.

$$P_{out}^n = \left[1 - \Pr\left(E_{n,1}^{sd} \cap \cdots \cap E_{n,n}^{sd}\right)\right] \times \left[1 - \Pr\left(E_{n,1}^{srd} \cap \cdots \cap E_{n,n}^{srd}\right)\right],$$
(25)

where $E_{n,j}^{srd}$ denotes D_n can successfully decode D_j's signal. Thus, $E_{n,j}^{srd}$ can be expressed as

$$E_{n,j}^{srd} = \{\gamma_{rd,j\to n} > \gamma_{thj}\}$$
(26)
$$= \left\{\rho_{rd_n} > \frac{\phi_{1,n}\gamma_{thj}}{c_2\gamma\left(a_j - \gamma_{thj}\left(\tilde{\Delta}_j + \Delta_j + d\right)\right)} \triangleq \psi_j, \right.$$
$$\left. \rho_{sr} > \frac{\varphi_j\left(\phi_{2,n}c_2\gamma\rho_{rd_n} + \phi_3\right)}{\phi_{1,n}c_1\gamma\left(\rho_{rd_n} - \varphi_j\right)}\right\},$$

where (26) follows from $a_j > \left(\tilde{\Delta}_j + \Delta_j + d\right)\gamma_{thj}$.

It is difficult to derive the exact expression for the OP of D_n due to high complexity of integral. We circumvent this problem by deriving the approximate expressions for the OP in the following theorem.

Theorem 2. *For $\alpha - \mu$ fading channels, the OPs of D_n can be approximated as*

---

[3]In this paper, we have the assumption that μ is an integer. For non-integer μ, we can obtain the approximate expression by flooring and ceiling.

- *Non-ideal conditions*

$$P_{out}^{n,\text{ni}} \approx \Xi \sum_{k=0}^{N-n} \binom{N-n}{k} \frac{(-1)^k}{n+k} \left(1 - \sum_{m_1=0}^{\mu_{sd_n}-1} \frac{e^{-\left(\frac{\theta_n^*}{\beta_{sd_n}}\right)^{\frac{\alpha_{sd_n}}{2}}}}{m_1!} \left(\frac{\theta_n^*}{\beta_{sd_n}}\right)^{\frac{\alpha_{sd_n}m_1}{2}}\right)^{n+k}$$

$$\times \left(1 - \sum_{m_2=0}^{\mu_{sr}-1} \sum_{m_3=0}^{\mu_{rd_n}-1} \frac{e^{-\left(\frac{\tau}{\beta_{sr}}\right)^{\frac{\alpha_{sr}}{2}} - \left(\frac{\psi_n^*}{\beta_{rd_n}}\right)^{\frac{\alpha_{rd_n}}{2}}}}{m_2!m_3!} \left(\frac{\tau}{\beta_{sr}}\right)^{\frac{\alpha_{sr}m_2}{2}} \left(\frac{\psi_n^*}{\beta_{rd_n}}\right)^{\frac{\alpha_{rd_n}m_3}{2}}\right), \quad (27)$$

where $\psi_n^* = \max\limits_{1 \le j \le n} \psi_j$, $\tau = \frac{c_2 \psi_n^* \phi_{2,n}}{c_1 \phi_{1,n}}$.

- *Ideal conditions*

$$P_{out}^{n,\text{id}} \approx \Xi \sum_{k=0}^{N-n} \binom{N-n}{k} \frac{(-1)^k}{n+k} \left(1 - \sum_{m_1=0}^{\mu_{sd_n}-1} \frac{e^{-\left(\frac{\vartheta_1}{\beta_{sd_n}}\right)^{\frac{\alpha_{sd_n}}{2}}}}{m_1!} \left(\frac{\vartheta_1}{\beta_{sd_n}}\right)^{\frac{\alpha_{sd_n}m_1}{2}}\right)^{n+k}$$

$$\times \left(1 - \sum_{m_2=0}^{\mu_{sr}-1} \sum_{m_3=0}^{\mu_{rd_n}-1} \frac{e^{-\left(\frac{\vartheta_2}{\beta_{sr}}\right)^{\frac{\alpha_{sr}}{2}} - \left(\frac{\vartheta_3}{\beta_{rd_n}}\right)^{\frac{\alpha_{rd_n}}{2}}}}{m_2!m_3!} \left(\frac{\vartheta_2}{\beta_{sr}}\right)^{\frac{\alpha_{sr}m_2}{2}} \left(\frac{\vartheta_3}{\beta_{rd_n}}\right)^{\frac{\alpha_{rd_n}m_3}{2}}\right), \quad (28)$$

where $\vartheta_2 = \max\limits_{1 \le j \le n} \frac{\gamma_{thj} d_{sr}^{\tilde{\alpha}}}{c_1 \gamma (a_j - \Delta_j \gamma_{thj})}$, $\vartheta_3 = \max\limits_{1 \le j \le n} \frac{\gamma_{thj} d_{rd_n}^{\tilde{\alpha}}}{c_2 \gamma (a_j - \Delta_j \gamma_{thj})}$.

Proof: See Appendix A. ∎

2) *Diversity Order:* Similarly, in order to obtain more insights, we focus on the asymptotic analysis in terms of diversity order at high SNR regime. By using (27) and (28), we observe that the asymptotic OP for the D_n at high SNRs in the following corollary.

Corollary 3. *At high SNRs ($\gamma \to \infty$), the asymptotic OP of D_n is given by*

- *Non-ideal conditions*

$$P_{out,\infty}^{n,\text{ni}} = \Xi' \frac{\left(\frac{\varsigma_1}{\beta_{sd_n}}\right)^{\frac{n\alpha_{sd_n}\mu_{sd_n}}{2}}}{(\mu_{sd_n}!)^n} \left(\frac{\left(\frac{\varsigma_2}{\beta_{sr}}\right)^{\frac{\alpha_{sr}\mu_{sr}}{2}}}{\mu_{sr}!} + \frac{\left(\frac{\varsigma_3}{\beta_{rd_n}}\right)^{\frac{\alpha_{rd_n}\mu_{rd_n}}{2}}}{\mu_{rd_n}!}\right), \quad (29)$$

where $\varsigma_2 = \max\limits_{1 \le j \le n} \frac{\gamma_{thj} d_{sr}^{\tilde{\alpha}} \sigma_{e_{sr}}^2 (1+d)}{(a_j - (\tilde{\Delta}_j + \Delta_j + d)\gamma_{thj})}$, $\varsigma_3 = \max\limits_{1 \le j \le n} \frac{\gamma_{thj} d_{rd_n}^{\tilde{\alpha}} \sigma_{e_{rd_n}}^2 (1+d)}{a_j - (\tilde{\Delta}_j + \Delta_j + d)\gamma_{thj}}$. *We note that* $\varsigma_2 = \max\limits_{1 \le j \le n} \frac{\gamma_{thj} d_{sr}^{\tilde{\alpha}} (1+d)}{\gamma_{sr}(a_j - (\tilde{\Delta}_j + \Delta_j + d)\gamma_{thj})}$, $\varsigma_3 = \max\limits_{1 \le j \le n} \frac{\gamma_{thj} d_{rd_n}^{\tilde{\alpha}} (1+d)}{\gamma_{rd_n}(a_j - (\tilde{\Delta}_j + \Delta_j + d)\gamma_{thj})}$ *when* $\sigma_{e_i}^2$ *is a function of SNR.*

- *Ideal conditions*

$$P_{out,\infty}^{n,\text{id}} = \Xi' \frac{\left(\frac{\vartheta_1}{\beta_{sd_n}}\right)^{\frac{n\alpha_{sd_n}\mu_{sd_n}}{2}}}{(\mu_{sd_n}!)^n} \left(\frac{\left(\frac{\vartheta_2}{\beta_{sr}}\right)^{\frac{\alpha_{sr}\mu_{sr}}{2}}}{\mu_{sr}!} + \frac{\left(\frac{\vartheta_3}{\beta_{rd_n}}\right)^{\frac{\alpha_{rd_n}\mu_{rd_n}}{2}}}{\mu_{rd_n}!}\right), \quad (30)$$

where $\Xi' = \frac{N!}{n!(N-n)!}$.

Proof: Taking the SNR into large ($\gamma \to \infty$), $F_{\rho_{sd_n}}(\theta_n^*)$, $F_{\rho_{sr}}(\tau)$ and $F_{\rho_{rd_n}}(\psi_n^*)$ can be respectively calculated as

$$F_{\tilde{\rho}_{sd_n}}(\theta_n^*) = \Xi' \frac{\left(\frac{\theta_n^*}{\beta_{sd_n}}\right)^{\frac{n\alpha_{sd_n}\mu_{sd_n}}{2}}}{(\mu_{sd_n}!)^n}, \quad F_{\rho_{sr}}(\tau) = \frac{\left(\frac{\tau}{\beta_{sr}}\right)^{\frac{\alpha_{sr}\mu_{sr}}{2}}}{\mu_{sr}!},$$

$$F_{\rho_{rd_n}}(\psi_n^*) = \frac{\left(\frac{\psi_n^*}{\beta_{rd_n}}\right)^{\frac{\alpha_{rd_n}\mu_{rd_n}}{2}}}{\mu_{rd_n}!}. \quad ∎$$

Next, the diversity orders are obtained in the following corollary.

Corollary 4. *The diversity orders for the OP of the n-th user are given by*

- *Non-ideal conditions: For fixed and variable estimation error model, the diversity orders can be given respectively by*

$$d_{2nd,f}^{n,\text{ni}} = 0, \quad (31)$$

$$d_{2nd,v}^{n,\text{ni}} = \min\left(\frac{n\alpha_{sd_n}\mu_{sd_n} + \alpha_{sr}\mu_{sr}}{2}, \frac{n\alpha_{sd_n}\mu_{sd_n} + \alpha_{rd_n}\mu_{rd_n}}{2}\right),$$

- *Ideal conditions*

$$d_{2nd}^{n,\text{id}} = \min\left(\frac{n\alpha_{sd_n}\mu_{sd_n} + \alpha_{sr}\mu_{sr}}{2}, \frac{n\alpha_{sd_n}\mu_{sd_n} + \alpha_{rd_n}\mu_{rd_n}}{2}\right). \quad (32)$$

Proof: By substituting (29) and (30) into (20), we can complete the proof after some simplifications. ∎

Remark 2. For ideal conditions, the outage performance is improved as the average SNR increasing. The diversity order is determined by the minimum value $(n\alpha_{sd_n}\mu_{sd_n} + \alpha_{sr}\mu_{sr})/2$ and $(n\alpha_{sd_n}\mu_{sd_n} + \alpha_{rd_n}\mu_{rd_n})/2$. For non-ideal conditions, when the estimation error is fixed, the asymptotic OP is a fixed constant, and results in zero diversity order. When $\sigma_{e_i}^2$ is a function of SNR, the diversity order is the same with ideal case since the channel can be accurately estimated in the high SNR regime.

IV. ERGODIC CAPACITY ANALYSIS

In this section, we analyze the EC performance for these two scenarios over $\alpha - \mu$ fading channels with hardware impairments and imperfect CSI, where the imperfect SIC is also taken into account.

A. Non-cooperative NOMA

1) EC: The achievable sum rate for the served users of the considered networks is obtained as

$$R_{\text{sum}}^{1st} = \sum_{n=1}^{N} \log_2(1 + \gamma_{sd_n}). \quad (33)$$

The EC can be expressed as

$$C_{\text{sum}} = \sum_{n=1}^{N} \mathbb{E}\{\log_2(1 + \gamma_{sd_n})\}. \quad (34)$$

Then, we focus on the approximate analysis since it is a great challenge to obtain an exact expression for the EC. The following theorem provides the approximate expressions for the EC.

Theorem 3. *For $\alpha - \mu$ fading channels, the approximate expressions for the EC can be expressed as*

- *Non-ideal conditions*

$$C_{\text{sum}}^{\text{ni}} \approx \sum_{n=1}^{N} \log_2\left(1 + \frac{a_n \gamma \chi_{sd_n}}{\gamma \Theta'_n \chi_{sd_n} + \varpi_{sd_n}}\right), \quad (35)$$

where $\chi_{sd_n} = \Xi \sum_{k=0}^{n-1} \binom{n-1}{k} \frac{(-1)^k \Gamma\left(\mu_{sd_n} + \frac{2}{\alpha_{sd_n}}\right)}{\Gamma(\mu_{rd_n})(N-n+k+1)^{\left(\mu_{sd_n} + \frac{2}{\alpha_{sd_n}}\right)}}$,
$\Theta'_n = \tilde{\Delta}_n + \Delta_n + \kappa_{sd_n}^2$, $\varpi_{sd_n} = d_{sd_n}^{\tilde{\alpha}}\left(\sigma_{e_{sd_n}}^2 \gamma\left(1+\kappa_{sd_n}^2\right) + 1\right)$.

- *Ideal conditions*

$$C_{\mathrm{sum}}^{\mathrm{id}} \approx \sum_{n=1}^N \log_2\left(1 + \frac{a_n\gamma\chi_{sd_n}}{\gamma\Delta_n\chi_{sd_n} + d_{sd_n}^{\tilde{\alpha}}}\right). \quad (36)$$

Proof: See Appendix B. ∎

In the following, we focus on the asymptotic analysis for the EC at high SNR regime, which can be used to analyze the *high SNR slope* and the *high SNR power offset*. The asymptotic expressions are given in the following corollary.

Corollary 5. *At high SNRs, the asymptotic EC expressions are given as*
- *Non-ideal conditions*

$$C_{\mathrm{sum}}^{\mathrm{ni},\infty} \approx \sum_{n=1}^N \log_2\left(1 + \frac{a_n\chi_{sd_n}}{\Theta'_n\chi_{sd_n} + \varpi'_{sd_n}}\right), \quad (37)$$

- *Ideal conditions*

$$C_{\mathrm{sum}}^{\mathrm{id},\infty} \approx \log_2\left(a_N\gamma\chi_{sd_N}\right). \quad (38)$$

where $\varpi'_{sd_n} = d_{sd_n}^{\tilde{\alpha}}\sigma_{e_{sd_n}}^2\left(1+\kappa_{sd_n}^2\right)$. We note that $\varpi'_{sd_n} = 0$ at high SNR regime when $\sigma_{sd_n}^2$ is a function of SNR.

Proof: Based on the analytical results in **Theorem 3**, after some simple manipulations, the asymptotic EC expressions can be obtained by considering $\gamma \to \infty$. ∎

2) High SNR Slope and high SNR Power Offset: To get deeper insights into EC performance at high SNRs, we aim to provide the high SNR analysis for the EC in terms of the *high-SNR slope* and the *high-SNR power offset*. We can write the asymptotic EC in a general form as [40, 41]

$$C_{\mathrm{sum}}^{\infty} = S_{\infty}\left(\log_2\gamma - \mathcal{L}_{\infty}\right) + o\left(1\right), \quad (39)$$

where γ is the average SNR, $\mathcal{S}_{\infty}$ and $\mathcal{L}_{\infty}$ are the *high-SNR slope* in bits/s/Hz(in 3 dB) and the *high-SNR power offset* in 3 dB units, respectively. The two metrics are defines as

$$S_{\infty} = \lim_{\gamma\to\infty}\frac{C_{\mathrm{sum}}}{\log_2\gamma}, \mathcal{L}_{\infty} = \lim_{\gamma\to\infty}\left(\log_2\gamma - \frac{C_{\mathrm{sum}}}{\mathcal{S}_{\infty}}\right). \quad (40)$$

Based on the derived results for the EC in (35) and (36), we aim to obtain the high SNR slope and power offset for non-ideal/ideal conditions.

Corollary 6. *The high SNR slope and the high SNR power offset for non-ideal/ideal conditions are obtained as*
- *Non-ideal conditions*

$$\mathcal{S}_{\infty}^{\mathrm{ni}} = 0, \mathcal{L}_{\infty}^{\mathrm{ni}} = \infty, \quad (41)$$

- *Ideal conditions*

$$\mathcal{S}_{\infty}^{\mathrm{id}} = 1, \mathcal{L}_{\infty}^{\mathrm{id}} = \log_2\frac{1}{a_N\chi_{sd_N}}. \quad (42)$$

Proof: By plugging (37) and (38) into (39) and (40) and after some manipulations, (41) and (42) can be attained. ∎

Remark 3. For non-ideal conditions, C_{sum} tends to a fixed value as the SNR approaches the infinity, resulting in a zero high SNR slope and an infinity high SNR power offset, which means that for high rate networks, the performance is limited by distortion noise and estimation error. For ideal condition, the high SNR slope is 1, which is irrelative to the fading parameters, distortion noise and estimation error. The high SNR power offset is a fixed constant, which only depends on $\log_2\frac{1}{a_N\chi_{sd_N}}$.

B. Cooperative NOMA

1) EC: As following the fact that target SINRs of the users are dominated by the users's channel condition. As previously mentioned $\tilde{\rho}_{sd_1} \leq \cdots \leq \tilde{\rho}_{sd_j} \leq \cdots \leq \tilde{\rho}_{sd_n} \leq \cdots \leq \tilde{\rho}_{sd_N}$, $\gamma_{sd_{j\to n}} \geq \gamma_{sd_j}$ is always holds but $\gamma_{rd_{j\to n}} \geq \gamma_{rd_j}$ may not correct when $\rho_{rd_n} \leq \rho_{rd_j}$. We consider selection combining at the users, the target SINRs of users can be given as $\gamma_{th_j} = \max\left(\gamma_{sd_j}, \gamma_{rd_j}\right)$. Therefore, the achievable date rate of D_n can be expressed as

$$R_n = \begin{cases} \frac{1}{2}\log_2\left(1 + \max\left(\gamma_{sd_n}, \gamma_{rd_n}\right)\right), & \text{if } \rho_{rd_n} > \rho_{rd_j} \\ \frac{1}{2}\log_2\left(1 + \gamma_{sd_n}\right), & \text{if } \rho_{rd_n} < \rho_{rd_j} \end{cases} \quad (43)$$

in which $\frac{1}{2}$ accounts for the fact that the whole communication process occupies two time slots.

Recalling that ρ_{rd_j} and ρ_{rd_n} are independent distributed random variables, we have $\mathrm{Pr}\left(\rho_{rd_j} > \rho_{rd_n}\right) = \mathrm{Pr}\left(\rho_{rd_j} < \rho_{rd_n}\right) = \frac{1}{2}$. From (43), the achievable sum rate of the considered networks is then obtained as

$$R_{\mathrm{sum}}^{2nd} = \sum_{n=1}^N \frac{1}{2}\left(\frac{1}{2}\log_2(1+\max(\gamma_{sd_n},\gamma_{rd_n})) + \frac{1}{2}\log_2(1+\gamma_{sd_n})\right). \quad (44)$$

Therefore, the EC of all the users can be expressed as

$$C_{\mathrm{sum}} = \sum_{n=1}^N \left(\frac{1}{2}\mathbb{E}\left\{\frac{1}{2}\log_2\left(1 + \max\left(\gamma_{sd_n}, \gamma_{rd_n}\right)\right)\right\} + \frac{1}{2}\mathbb{E}\left\{\frac{1}{2}\log_2\left(1 + \gamma_{sd_n}\right)\right\}\right). \quad (45)$$

Now, we focus on the approximate analysis since it is challenging to obtain an exact expression for the EC. The following theorem provides the approximate expressions for the EC over $\alpha - \mu$ fading channels.

Theorem 4. *For $\alpha - \mu$ fading channels, the approximate closed-form expressions for the EC of users can be expressed as*
- *Non-ideal conditions*
For non-ideal conditions, the approximation expression for the EC of users in (46) is at the top of next page.
- *Ideal conditions*
For ideal conditions, the approximation expression for the EC of users in (47) is at the top of next page.
where $\Theta''_n = \tilde{\Delta}_n + \Delta_n + d$, $\chi_I = \frac{\Gamma\left(\mu_I + \frac{2}{\alpha_I}\right)}{\Gamma(\mu_I)}, I = sr, rd_n$.

Proof: See Appendix C. ∎

$$C_{\text{sum}}^{\text{ni}} \approx \frac{1}{4} \sum_{n=1}^{N} \left(\log_2 \left(1 + \max \left(\frac{a_n \gamma \chi_{sd_n}}{\gamma \Theta'_n \chi_{sd_n} + \varpi_{sd_n}}, \frac{a_n c_1 c_2 \gamma^2 \chi_{sr} \chi_{rd_n}}{c_1 c_2 \gamma^2 \Theta''_n \chi_{sr} \chi_{rd_n} + c_1 \gamma \phi_{1,n} \chi_{sr} + c_2 \gamma \phi_{2,n} \chi_{rd_n} + \phi_{3,n}} \right) \right) \right.$$
$$\left. + \log_2 \left(1 + \frac{a_n \gamma \chi_{sd_n}}{\gamma \Theta'_n \chi_{sd_n} + \varpi_{sd_n}} \right) \right), \tag{46}$$

$$C_{\text{sum}}^{\text{id}} \approx \frac{1}{4} \sum_{n=1}^{N} \left(\log_2 \left(1 + \max \left(\frac{a_n \gamma \chi_{sd_n}}{\gamma \left(\tilde{\Delta}_n + \Delta_n \right) \chi_{sd_n} + d_{sd_n}^{\tilde{\alpha}}}, \frac{a_n c_1 c_2 \gamma^2 \chi_{sr} \chi_{rd_n}}{c_1 c_2 \gamma^2 \left(\tilde{\Delta}_n + \Delta_n \right) \chi_{sr} \chi_{rd_n} + c_1 \gamma d_{rd_n}^{\tilde{\alpha}} \chi_{sr} + c_2 \gamma d_{sr}^{\tilde{\alpha}} \chi_{rd_n} + d_{sr}^{\tilde{\alpha}} d_{rd_n}^{\tilde{\alpha}}} \right) \right) \right.$$
$$\left. + \log_2 \left(1 + \frac{a_n \gamma \chi_{sd_n}}{\gamma \left(\tilde{\Delta}_n + \Delta_n \right) \chi_{sd_n} + d_{sd_n}^{\tilde{\alpha}}} \right) \right), \tag{47}$$

TABLE I: Diversity order (DO), high SNR slope (HSS) and high SNR power offset (HSP) for the two scenarios

Scenarios	Hardware	DO	HSS	HSP
First	Ideal	$\frac{n\alpha_{sd_n}\mu_{sd_n}}{2}$	1	$\log_2 \left(\frac{1}{a_N \chi_{sd_N}} \right)$
	Non-ideal	0(1st) ; $\frac{n\alpha_{sd_n}\mu_{sd_n}}{2}$ (2nd)	0	∞
Second	Ideal	$\min \left(\frac{n\alpha_{sd_n}\mu_{sd_n}+\alpha_{sr}\mu_{sr}}{2}, \frac{n\alpha_{sd_n}\mu_{sd_n}+\alpha_{rd_n}\mu_{rd_n}}{2} \right)$	$\frac{1}{2}$	$\log_2 \left(\frac{1}{\max\left(a_N\chi_{sd_N},a_N\sqrt{\frac{\chi_{sd_N}\chi_{sr}\chi_{rd_N}}{(\chi_{sr}+\chi_{rd_N})}}\right)} \right)$
	Non-ideal	0(1st) ; $\min\left(\frac{n\alpha_{sd_n}\mu_{sd_n}+\alpha_{sr}\mu_{sr}}{2}, \frac{n\alpha_{sd_n}\mu_{sd_n}+\alpha_{rd_n}\mu_{rd_n}}{2}\right)$ (2nd)	0	∞

To obtain insightful expressions, we focus on the asymptotic analysis for the EC at high SNR regimes. The asymptotic expressions are given in the following corollary.

Corollary 7. *At high SNRs, the asymptotic expressions for EC are given as*
• *Non-ideal conditions*
For non-ideal conditions, the asymptotic expression for the EC is given as (48) *at the top of the next page.*
where $\phi'_{1,n} = d_{rd_n}^{\tilde{\alpha}} c_2 \sigma_{erd_n}^2 (1+d)$, $\phi'_2 = d_{sr}^{\tilde{\alpha}} c_1 \sigma_{esr}^2 (1+d)$, $\phi'_{3,n} = d_{sr}^{\tilde{\alpha}} d_{rd_n}^{\tilde{\alpha}} c_1 c_2 \sigma_{esr}^2 \sigma_{erd_n}^2 (1+d)$, $\varpi'_{sd_n} = d_{sd_n}^{\tilde{\alpha}} \sigma_{esd_n}^2 \left(1 + \kappa_{sd_n}^2 \right)$. *Note that* $\phi'_{1,n} = 0$, $\phi'_2 = 0$, $\phi'_{3,n} = 0$, $\varpi'_{sd_n} = 0$ *at high SNRs when* $\sigma_{e_i}^2$ *is a function of SNR.*
• *Ideal conditions*
For ideal conditions, the asymptotic expression for the EC is given as (49) *at the top of the next page.*

2) High SNR Slope and High Power Offset: Based on the results of (46) and (47), the *high SNR slope* and *high SNR power offset* are obtained in the following corollary.

Corollary 8. *The* high SNR slope *and the* high SNR power offset *for non-ideal/ideal conditions are obtained as*
• *Non-ideal conditions*

$$\mathcal{S}_\infty^{\text{ni}} = 0, \mathcal{L}_\infty^{\text{ni}} = \infty, \tag{50}$$

• *Ideal conditions*

$$\mathcal{S}_\infty^{\text{id}} = \frac{1}{2},$$
$$\mathcal{L}_\infty^{\text{id}} = \log_2 \frac{1}{\max \left(a_N \chi_{sd_N}, a_N \sqrt{\frac{\chi_{sd_N}\chi_{sr}\chi_{rd_N}}{\chi_{sr}+\chi_{rd_N}}} \right)}. \tag{51}$$

Proof: By plugging (46) and (47) into (39) and (40), after some manipulations, (50) and (51) can be attained. ∎

Remark 4. For non-ideal conditions, C_{sum} tends to a fixed constant as the SNR approaches the infinity, resulting in zero *high SNR slope* and infinity *high SNR power offset*, which means that for high rate networks, the performance is limited by distortion noise and estimation error. For ideal condition, the high SNR slope is $\frac{1}{2}$, which is irrelative to the fading parameters, distortion noise and estimation error. The high SNR power offset is fixed constant, which only depends on $\log_2 \frac{1}{\max \left(a_N \chi_{sd_N}, a_N \sqrt{\frac{\chi_{sd_N}\chi_{sr}\chi_{rd_N}}{\chi_{sr}+\chi_{rd_N}}} \right)}$.

As shown in Table I, the diversity order, *high SNR slope* and *high SNR power offset* are summarized to illustrate the comparison. For convenience, we use "DO", "HSS" and "HSP" to denote diversity order, high SNR slope and high SNR power offset, respectively.

V. RELAY LOCATION OPTIMIZATION

In this section, our objective is to find the optimal location of relay R for cooperative NOMA scenario with the asymptotic OP. We consider an one-dimensional linear topology network, where the S, R and D_n stand in a line and R is on the line between the S and D_n. Then, we have $d_{sd_n} = d_{sr} + d_{rd_n}$. The relay location ratio is defined as $\zeta = d_{sr}/d_{sd_n}$. We formulate the optimal relay location problem based on the minimize asymptotic OP.

Problem Formulation: For given sum distance d_{sd_n}, $d_{sr} = \zeta d_{sd_n}$, $d_{rd_n} = (1 - \zeta) d_{sd_n}$, the optimal relay location

$$C_{\text{sum}}^{\text{ni},\infty} \approx \frac{1}{4} \sum_{n=1}^{N} \left(\log_2 \left(1 + \max \left(\frac{a_n \chi_{sd_n}}{\Theta'_n \chi_{sd_n} + \varpi'_{sd_n}}, \frac{a_n \chi_{sr} \chi_{rd_n}}{\Theta''_n \chi_{sr} \chi_{rd_n} + \phi'_{1,n} \chi_{sr} + \phi'_2 \chi_{rd_n} + \phi'_{3,n}} \right) \right) + \log_2 \left(1 + \frac{a_n \chi_{sd_n}}{\Theta'_n \chi_{sd_n} + \varpi'_{sd_n}} \right) \right), \quad (48)$$

$$C_{\text{sum}}^{\text{id},\infty} \approx \frac{1}{4} \left(\log_2 \left(\max \left(a_N \gamma \chi_{sd_N}, \frac{a_N \gamma \chi_{sr} \chi_{rd_N}}{\chi_{sr} + \chi_{rd_N}} \right) \right) + a_N \gamma \chi_{sd_N} \right). \quad (49)$$

ratio ζ^* is reduced to

$$\begin{aligned} &\text{minimize } P_{out,\infty}^{n,\text{ni}}(\zeta) \\ &\text{subject to } 1 \geq \zeta \geq 0 \end{aligned} \quad (52)$$

Then the asymptotic expression of OP in Corollary 3 can be rewritten in terms of the ratio ζ as

$$P_{out,\infty}^n(\zeta) = \Xi' X_{sd_n} \quad (53)$$

$$\times \left(\zeta^{\frac{\alpha_{sr} \mu_{sr} \tilde{\alpha}}{2}} \frac{\left(\frac{X_{sr}}{\beta_{sr}} \right)^{\frac{\alpha_{sr} \mu_{sr}}{2}}}{\mu_{sr}!} + (1-\zeta)^{\frac{\alpha_{rd_n} \mu_{rd_n} \tilde{\alpha}}{2}} \frac{\left(\frac{X_{rd_n}}{\beta_{rd_n}} \right)^{\frac{\alpha_{rd_n} \mu_{rd_n}}{2}}}{\mu_{rd_n}!} \right),$$

For ideal conditions, $X_{sd_n} = \frac{(\vartheta_1/\beta_{sd_n})^{\frac{n\alpha_{sd_n}\mu_{sd_n}}{2}}}{(\mu_{sd_n}!)^n}$, $X_{sr} = d_{sd_n}^{\tilde{\alpha}} \max_{1 \leq j \leq n} \frac{\gamma_{thj}}{c_1 \gamma(a_j - (\tilde{\Delta}_j + \Delta_j)\gamma_{thj})}$, $X_{rd_n} = d_{sd_n}^{\tilde{\alpha}} \max_{1 \leq j \leq n} \frac{\gamma_{thj}}{c_2 \gamma(a_j - (\tilde{\Delta}_j + \Delta_j)\gamma_{thj})}$; For non-ideal conditions, $X_{sd_n} = \frac{(\varsigma_1/\beta_{sd_n})^{\frac{n\alpha_{sd_n}\mu_{sd_n}}{2}}}{(\mu_{sd_n}!)^n}$, $X_{sr} = d_{sd_n}^{\tilde{\alpha}} \max_{1 \leq j \leq n} \frac{\gamma_{thj}\sigma_{e_{sr}}^2(1+d)}{a_j - (\tilde{\Delta}_j + \Delta_j + d)\gamma_{thj}}$, $X_{rd_n} = d_{sd_n}^{\tilde{\alpha}} \max_{1 \leq j \leq n} \frac{\gamma_{thj}\sigma_{e_{rd_n}}^2(1+d)}{a_j - (\tilde{\Delta}_j + \Delta_j + d)\gamma_{thj}}$.

To minimize the asymptotic OP of (53) in terms of the ratio ζ, it can be simplified to minimize the following term

$$f(\zeta) = \zeta^{\frac{\alpha_{sr}\mu_{sr}\tilde{\alpha}}{2}} \frac{\left(\frac{X_{sr}}{\beta_{sr}} \right)^{\frac{\alpha_{sr}\mu_{sr}}{2}}}{\mu_{sr}!} + (1-\zeta)^{\frac{\alpha_{rd_n}\mu_{rd_n}\tilde{\alpha}}{2}} \frac{\left(\frac{X_{rd_n}}{\beta_{rd_n}} \right)^{\frac{\alpha_{rd_n}\mu_{rd_n}}{2}}}{\mu_{rd_n}!}, \quad (54)$$

We first prove that the function $f(\zeta)$ is convex with respect to ζ.

Lemma 1. *The optimal relay location ratio ζ^* which minimizes the asymptotic OP in Corollary 3 is unique with fixed power allocation.*

Proof: The second derivative of function $f(\zeta)$ with respect to ζ can be derived as

$$f''(\zeta) = \frac{\alpha_{sr}\mu_{sr}\tilde{\alpha}}{2} \left(\frac{\alpha_{sr}\mu_{sr}\tilde{\alpha}}{2} - 1 \right) \zeta^{\frac{\alpha_{sr}\mu_{sr}\tilde{\alpha}}{2} - 2} \frac{\left(\frac{X_{sr}}{\beta_{sr}} \right)^{\frac{\alpha_{sr}\mu_{sr}}{2}}}{\mu_{sr}!} \quad (55)$$

$$+ \frac{\alpha_{rd_n}\mu_{rd_n}\tilde{\alpha}}{2} \left(\frac{\alpha_{rd_n}\mu_{rd_n}\tilde{\alpha}}{2} - 1 \right) (1-\zeta)^{\frac{\alpha_{rd_n}\mu_{rd_n}\tilde{\alpha}}{2} - 2} \frac{\left(\frac{X_{rd_n}}{\beta_{rd_n}} \right)^{\frac{\alpha_{rd_n}\mu_{rd_n}}{2}}}{\mu_{rd_n}!}.$$

We note that $f''(\zeta) > 0$ for $\zeta \in [0,1]$ in (55), which implies that the first derivative $f'(\zeta)$ is a increasing function. Since $f'(0) < 0$, $f'(1) > 0$, thus $f'(\zeta)$ is convex with respect to ζ, i.e., $f'(\zeta) = 0$ has a unique solution in the interval $[0,1]$. ∎

Therefore, the optimal relay location ratio ζ^* can be obtained by solving the derivation of $f(\zeta)$ as follows

$$f'(\zeta) = \frac{\alpha_{sr}\mu_{sr}\tilde{\alpha}}{2} \zeta^{\frac{\alpha_{sr}\mu_{sr}\tilde{\alpha}}{2} - 1} \frac{\left(\frac{X_{sr}}{\beta_{sr}} \right)^{\frac{\alpha_{sr}\mu_{sr}}{2}}}{\mu_{sr}!} \quad (56)$$

$$- \frac{\alpha_{rd_n}\mu_{rd_n}\tilde{\alpha}}{2} (1-\zeta)^{\frac{\alpha_{rd_n}\mu_{rd_n}\tilde{\alpha}}{2} - 1} \frac{\left(\frac{X_{rd_n}}{\beta_{rd_n}} \right)^{\frac{\alpha_{rd_n}\mu_{rd_n}}{2}}}{\mu_{rd_n}!} = 0,$$

It is intractable to obtain the closed-from solution of the equation of (56), if not impossible. In the following, the channels $\hat{g}_{sr}$ and $\hat{g}_{rd_n}$ are assumed to be independent identically distributed, i.e., $\alpha_{sr} = \alpha_{rd_n} = \alpha$, $\mu_{sr} = \mu_{rd_n} = \mu$, $\beta_{sr} = \beta_{rd_n} = \beta$, in order to obtain deeper insights on the optimal relay location ratio ζ^*.

Theorem 5. *Assuming that the channels $\hat{g}_{sr}$ and $\hat{g}_{rd_n}$ are independent identically distributed, the optimal relay location ratio ζ^* can be obtained as*

$$\zeta^* = \frac{1}{1 + \left(\frac{X_{sr}}{X_{rd_n}} \right)^{\frac{1}{\tilde{\alpha} - \frac{2}{\alpha\mu}}}}. \quad (57)$$

for ideal conditions, $X_{sr}/X_{rd_n} = c_2/c_1$; for non-ideal conditions, $X_{sr}/X_{rd_n} = \sigma_{e_{sr}}^2 / \sigma_{e_{rd_n}}^2$.

Remark 5. From (57), we can observe that the optimal relay location ratio ζ^* is determined by c_1, c_2, α, μ and $\tilde{\alpha}$ for ideal conditions, the optimal relay location ratio can be derived as $\zeta^* = \frac{1}{2}$ when $c_1 = c_2$. However, it is determined by $\sigma_{e_{sr}}^2$, $\sigma_{e_{rd_n}}^2$, α, μ and $\tilde{\alpha}$ for non-ideal conditions. ζ^* is $\frac{1}{2}$ when $\sigma_{e_{sr}}^2 = \sigma_{e_{rd_n}}^2$.

VI. ENERGY EFFICIENCY

EE has been as an important criteria to evaluate the performance of wireless communication systems, which is defined as the bits of information reliably transferred the receivers per unit consumed energy at the transmitters [20]

$$\nu_{EE} = \frac{\text{Total date rate}}{\text{Total energy consumption}}. \quad (58)$$

where the total date rate is the sum rate, whereas the total power consumption denotes the sum of the transmitted power.

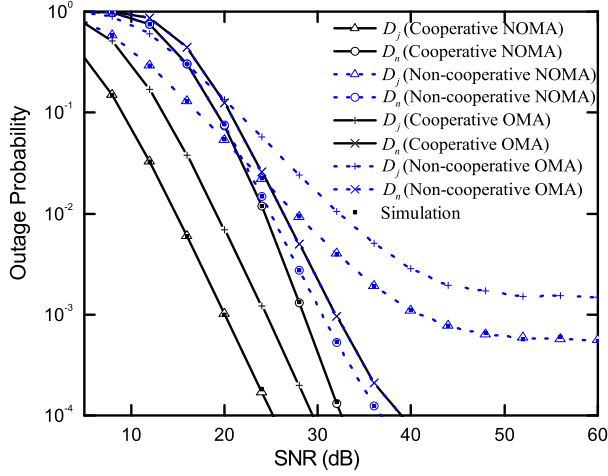Next, we analyze the EE of two different scenarios in the following theorem.

Fig. 2: The OP of the users for the two scenarios versus SNR

Fig. 3: The OP of the users for the two scenarios versus SNR

A. non-cooperative NOMA

Theorem 6. *The EE of the proposed networks for non-cooperative NOMA is expressed as*

$$\nu_{EE} = \frac{2R_{\text{sum}}^{1st}}{TP_s}, \qquad (59)$$

where T denotes the transmission time for the entire communication process, while R_{sum}^{1st} can be obtained from (33).

B. cooperative NOMA

Theorem 7. *The EE of the proposed networks for non-cooperative NOMA is expressed as*

$$\nu_{EE} = \frac{2R_{\text{sum}}^{2nd}}{T(P_s + P_r)}, \qquad (60)$$

where R_{sum}^{2nd} can be obtained from (44).

VII. NUMERICAL RESULT

In this section, some numerical results are provided to validate the accuracy of the theoretical analyses for the considered two scenarios. Complementary performance evaluation results obtained by means of Monte Carlo computer simulation trials will also be presented in order to confirm the accuracy of the theoretical approach and the analytical results. Hereinafter, unless other specified, specific values for the various system parameters are assumed as follows: $\alpha_i = 2$, $\mu_i = 1$, $c_1 = c_2 = 1$, $N = 2$, $j = 1$, $n = 2$, $\gamma_{th_j} = 2$dB and $\gamma_{th_n} = 5$dB, $a_j = 7/8$, $a_n = 1/8$, $d_{sd_j} = 1$m, $d_{sd_n} = 0.8$m, $d_{sr} = 0.1$m, $d_{rd_j} = d_{sd_j} - d_{sr} = 0.9$m, $d_{rd_n} = d_{sd_n} - d_{sr} = 0.7$m, $\tilde{\alpha} = 4$. In the following simulation, we assume that the systems have the imperfect but good SIC performance with small value $\xi_1 = 0.005$. Also, in the simulation, two different types of channel estimate error are considered: 1) fixed $\sigma_{e_i}^2$, and 2) $\sigma_{e_i}^2$ is a function of $\sigma_{e_i}^2 = \Omega_i/(1 + \delta\gamma\Omega_i)$.

Fig. 2 shows the OP of the users for the two scenarios versus SNR, obtained by cooperative NOMA and non-cooperative NOMA, with $\sigma_{e_i} = 0.01$, $\kappa_i = 0.1$, $\xi_1 = 0.005$. Moreover, cooperative orthogonal multiple access (OMA) and non-cooperative OMA curves are provided for the purpose of
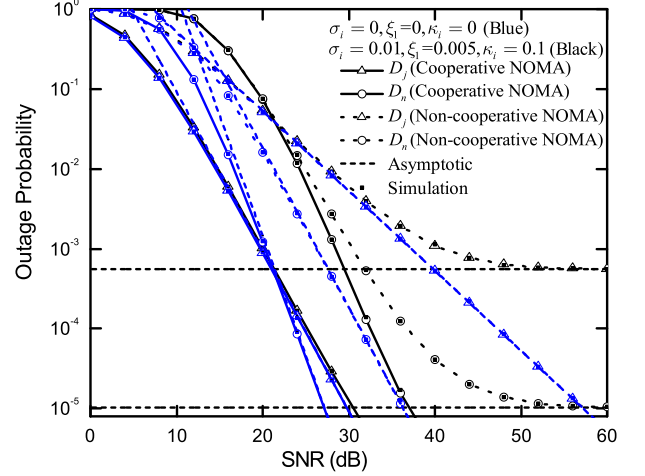
comparison. The target rate for the orthogonal user γ_{th_0} is set to $\gamma_{th_0} = \sum_{n=1}^{N} \gamma_{th_n}$ bit per channel user (BPCU). The exact OP curves of the users for non-cooperative NOMA are given by Monte-Carlo simulation and perfectly match with the analytical results derived in (17). The approximate OP curves of the users for cooperative NOMA are also given by (27) and well approximate the Monte-Carlo simulation curves. Additionally, we can observe that NOMA is capable of the outperforming OMA in terms of OP.

Fig. 3 shows the OP of the users for the two scenarios versus the SNR with $\{\sigma_{e_i}, \xi_1, \kappa_i\} = \{0, 0, 0; 0.01, 0.005, 0.1\}$. For the ideal conditions $\{\sigma_{e_i}, \xi_1, \kappa_i\} = \{0, 0, 0\}$, the exact and asymptotic OP curves are plotted according to (17), (18) and (21), (22), respectively. For the non-ideal conditions $\{\sigma_{e_i}, \xi_1, \kappa_i\} = \{0.01, 0.005, 0.1\}$, the lower bounds and asymptotic results for the OP are derived by (27), (28) and (29), (30), respectively. We can observe that the theoretical analyses match precisely with simulation results across the entire SNRs. Moreover, the OP approaches a fixed constant when the average SNR grows into infinity due to the fixed estimation error, which results in zero diversity order. These results verify the conclusion in Remark 1 and Remark 2. Comparing with two scenarios above, cooperative NOMA provides better outage performance than non-cooperative NOMA one due to the extra cooperative diversity gain.

Fig. 4 presents the OP of the users for the two scenarios versus SNR with $\delta = \{0.2, 0.5, 1\}$. In this simulation, we set $\kappa_i = 0$, $\xi_1 = 0.005$. One can observe that the OP increases as δ decreases at a positive finite δ. This means that smaller δ causes larger estimation error and results in severe performance loss. Moreover, as expected, better channel estimation quality (large δ) can significantly improve the outage performance for all user. Finally, we can also observe that NOMA can enhance the fairness between near user and far user by allocating more power to the far user.

Fig. 5 plots the OP of the users for the two scenarios versus SNR for varying $\alpha = \{2, 3, 4\}$. We assume $\mu_i = 1$, $\sigma_{e_i} = 0.01$, $\kappa_i = 0.1$, $\xi_1 = 0.005$. We can observe that the OP of the users for a larger α outperforms that of smaller one, which
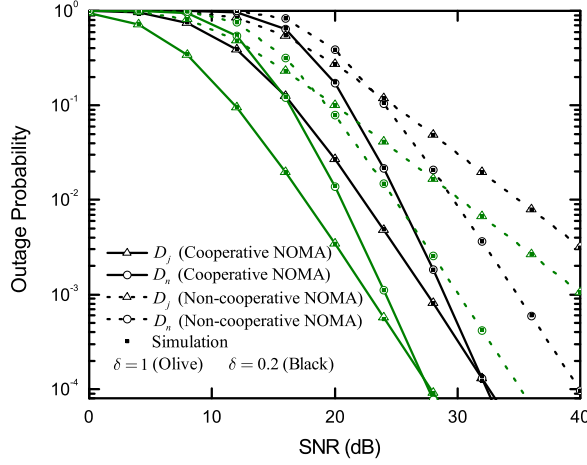
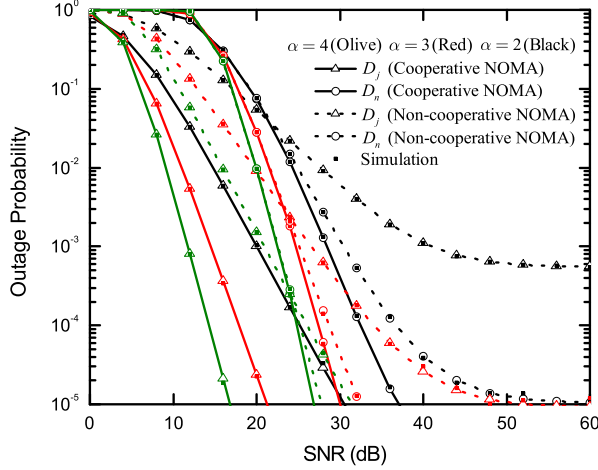Fig. 4: The OP of the users for the two scenarios versus SNR for different δ

Fig. 5: The OP of the users for the two scenarios versus SNR for different α

Fig. 6: The OP of the users for the two scenarios versus SNR

Fig. 7: The OP of the users for the two scenarios versus d_{sr}

means that the nonlinearity of $\alpha - \mu$ fading channels can be exploited to improve outage performance. In addition, for non-ideal conditions, there exist error floors of OP due to the fixed estimation error, which is consistent with the analytical result of Corollary 4.

Fig. 6 plots the OP of the users for the two scenarios versus SNR with three different cases: *i)* $\sigma_{e_i}^2 = 0, \xi_1 = 0, \kappa_i = 0$; *ii)* $\sigma_{e_i}^2 = 0, \xi_1 = 0.005, \kappa_i = 0.1$; *iii)* $\sigma_{e_i}^2 = \frac{\Omega_i}{1 + \delta\gamma\Omega_i}, \xi_1 = 0.005, \kappa_i = 0$ with $\delta = 1$. A specific observation is that the far user is more sensitive to the distortion noise than the near user, while estimation error is of significant to outage performance of the users due to inaccurate CSI. In addition, the differences of OP between ideal conditions and non-ideal conditions are almost ignored at low SNRs.

Fig. 7 plots the OP of the users for the two scenarios versus d_{sr} with $d_{sd_j} = 10$m, $d_{sd_n} = 8$m, $d_{rd_j} = d_{sd_j} - d_{sr}$, $d_{rd_n} = d_{sd_n} - d_{sr}$. The path loss parameter is set as $\tilde{\alpha} = 3$. Additionally, we set $\sigma_{e_i} = 0$, $\xi_1 = 0$, $\kappa_i = 0$ and $\sigma_{e_i} = 0.01$,
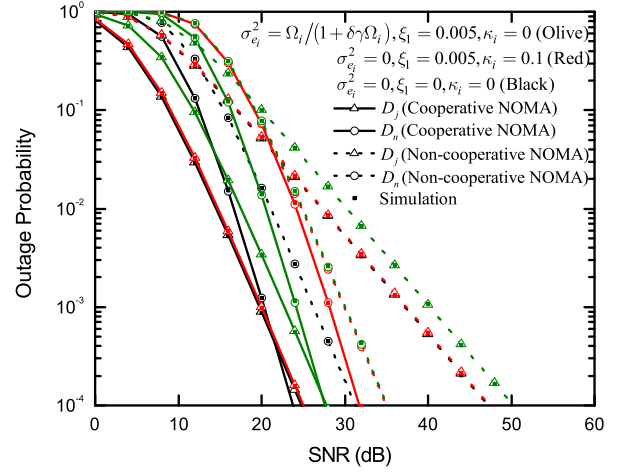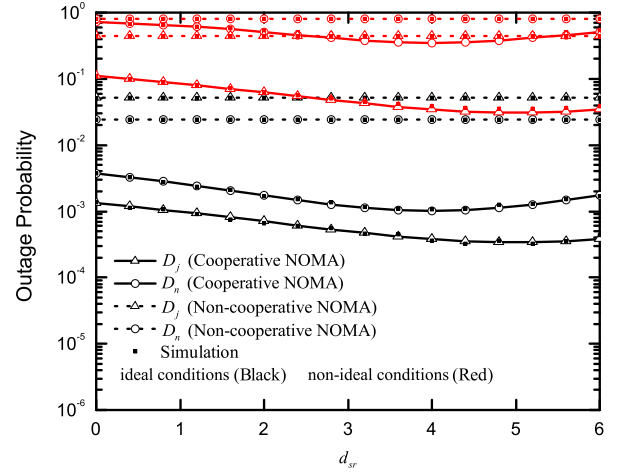
$\xi_1 = 0.005$, $\kappa_i = 0.01$ for ideal and non-ideal conditions, respectively. For ideal conditions, we can observe that D_j have better outage performance when $d_{sr} \approx 5$m, D_n have better outage performance when $d_{sr} \approx 4$m. This is because that the optimal relay location ratio is obtained as $\zeta^* = 1/2$ when $c_1 = c_2$, which is consistent with the result of Remark 5. For non-ideal conditions, we can also observe that D_j have better outage performance when $d_{sr} \approx 5$m, D_n have better outage performance when $d_{sr} \approx 4$m. This can be explained by the fact that the optimal relay location ratio is $\zeta^* = 1/2$ when $\sigma_{e_{sr}} = \sigma_{e_{rd_n}}$, which is also consistent with the result of Remark 5.

Fig. 8 plots the approximate EC of the users for the two scenarios versus the SNR with different relay positions; these curves are obtained using (35), (37), (46) and (48). We set $\alpha_i = 9$, $\mu_i = 1$, $d_{sr} = \{0.5\text{m}, 4.5\text{m}\}$, $d_{sd_j} = 10$m, $d_{sd_n} = 8$m, $d_{rd_j} = d_{sd_j} - d_{sr}$, $d_{rd_n} = d_{sd_n} - d_{sr}$, $\tilde{\alpha} = 4$, $\sigma_{e_i} = 0.01$, $\xi_1 = 0.005$, $\kappa_i = 0.1$. Comparing Fig. 8 (a) and 8 (b), it can be observed that when $d_{sr} = 0.5$m, i.e., the relay is nearer to the BS, non-cooperative NOMA provides better performance than that of cooperative NOMA; when $d_{sr} = 4.5$m, cooperative NOMA outperforms the non-cooperative NOMA,
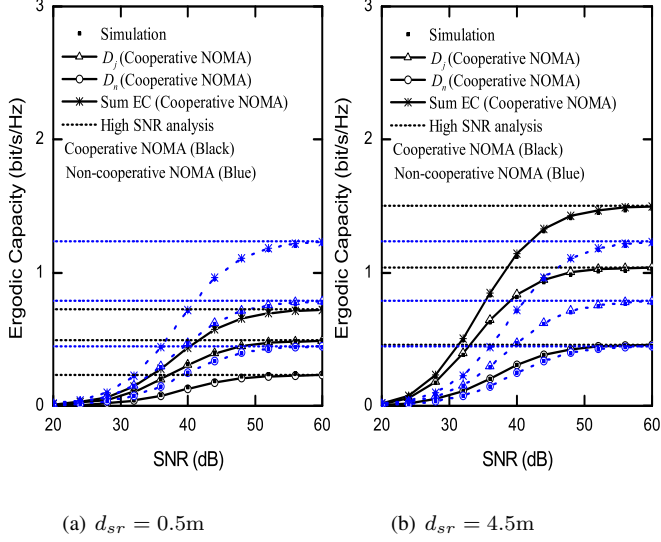
(a) $d_{sr} = 0.5$m   (b) $d_{sr} = 4.5$m

Fig. 8: The EC of the users for the two scenarios versus the SNR with different relay positions

Fig. 9: The EC of the users for the two scenarios versus

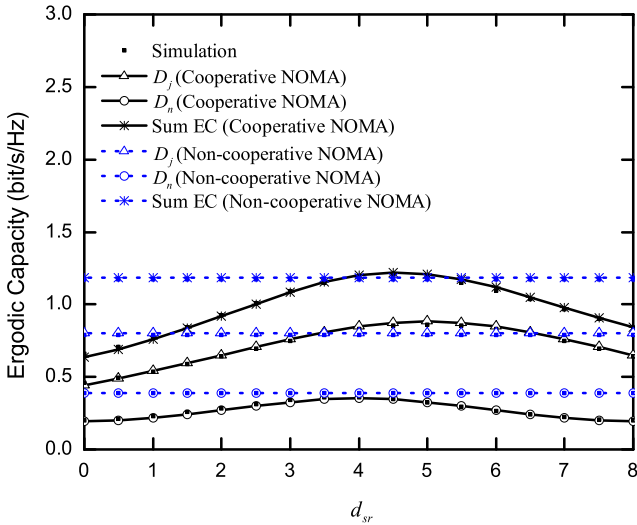Fig. 10: The EC of the users for the two scenarios versus κ_{sr}

Fig. 11: The EC of the users for the two scenarios versus $\sigma_{e_{sr}}$

which is intuitive. This means that by carefully selecting the relay location between source and destination, the EC of the cooperative NOMA can be maximized.

Fig. 9 plots the approximate EC of the users for the two scenarios versus d_{sr} with $d_{sd_j} = 10$m, $d_{sd_n} = 8$m, $d_{rd_j} = d_{sd_j} - d_{sr}$, $d_{rd_n} = d_{sd_n} - d_{sr}$. In this simulation, parameter values are set $\tilde{\alpha} = 3$, $\sigma_{e_i} = 0$, $\xi_1 = 0$, $\kappa_i = 0$. We can observe that when the relay is nearer to the BS or the users, non-cooperative NOMA outperform cooperative NOMA, otherwise cooperative NOMA provides better performance than non-cooperative. When d_{sr} is about 4.5m, i.e., the position of the relay lies in the middle between the BS and the users, we can also observe that in this point, cooperative NOMA achieves the optimal performance, which is consistent with the results of Fig. 8.
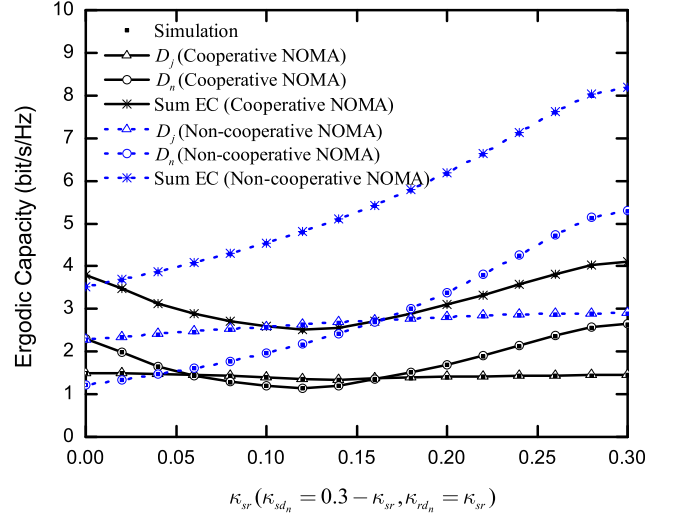
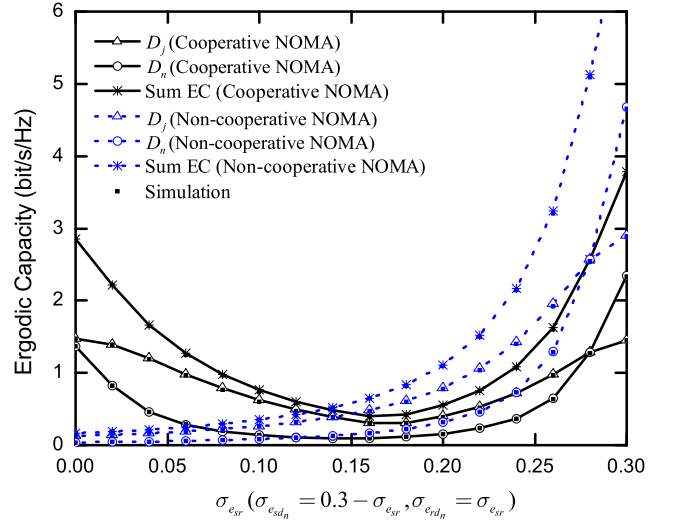Fig. 10 shows the EC for the two scenarios versus hardware impairments κ_{sr} with $\sigma_i = 0$, $\xi_1 = 0$. The distances is set as $d_{sr} = 4.5$, $d_{sd_j} = 10$m, $d_{sd_n} = 8$m, the path loss parameter is $\tilde{\alpha} = 4$. The hardware impairments parameters $\kappa_{rd_n}, \kappa_{sd_n}$ are selected to yield $\kappa_{rd_n} = \kappa_{sr}$ and $\kappa_{sr} + \kappa_{sd_n} = 0.3$.[4] One can observe that the EC for cooperative NOMA first decreases and then increases with the increases of κ_{sr}. However, the EC for non-cooperative NOMA increases with κ_{sr} increases. This is due to the fact that when κ_{sr} increases, the relay links has serious hardware impairments, the direct link has small hardware impairments.

Fig. 11 shows the EC for the two scenarios versus estimation error σ_{e_i} with $\kappa_i = 0$, $\xi_1 = 0$. The distance is set as $d_{sr} = 4.5$, $d_{sd_j} = 10$m, $d_{sd_n} = 8$m, the path loss parameter is $\tilde{\alpha} = 2$. The estimation error parameters $\sigma_{e_{rd_n}}$ and $\sigma_{e_{sd_n}}$ are obtained according to $\sigma_{e_{rd_n}} = \sigma_{e_{sr}}$ and $\sigma_{e_{sr}} + \sigma_{e_{sd_n}} = 0.3$. We can observe that the EC for cooperative NOMA is better

---

[4]As stated in [38], the typical value of κ is [0.08,0.175]. For the purpose of comparison, we set the arrange of summation $\kappa_{sr} + \kappa_{sd_n}$ is [0, 0.3].
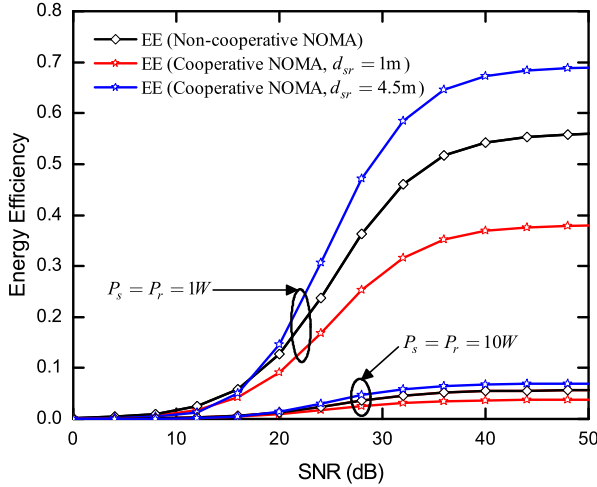
Fig. 12: The EE of the considered networks for two scenarios versus SNR

than that of non-cooperative NOMA when $\sigma_{e_{sr}}$ is small. This can be explained that when $\sigma_{e_{sr}}$ is small, the direct link has serious estimation error. Also, this figure shows the user communicates with BS according to the direct link for cooperative NOMA when $\sigma_{e_{sr}}$ is larger.

Fig. 12 plots the EE of the two scenarios with two different relay location: i) $d_{sr} = 1$m; ii) $d_{sr} = 4.5$m. In this simulation, we set $\kappa_i = 0.05$, $\xi_1 = 0.005$, $\sigma_{e_i} = 0.05$, $d_{sd_j} = 10$m, $d_{sd_n} = 8$m, and $T = 1$. The curves for cooperative/non-cooperative NOMA are obtained from (59) and (60), respectively. We can observe that the cooperative NOMA scenario with $d_{sr} = 4.5$m has a higher EE compared to non-cooperative NOMA at high SNR region. However, the non-cooperative NOMA scenario outperform cooperative NOMA scenario with $d_{sr} = 1$m at high SNR region. The reason is that the total rate date is maximize when the relay located in the middle between the BS and the users.

VIII. CONCLUSION

In this paper, we analyzed the performance of cooperative NOMA networks over over $\alpha - \mu$ fading channels, where three realistic factors are taken into account, namely RTHIs, imperfect CSI and imperfect SIC. Two typical scenarios were considered insightfully. The analytical expressions for the OP and EC for the two scenarios were derived. For the first estimation model, owing to the channel estimation error, there are error floors for the OP, and the diversity order for the two scenarios are 0. For the second estimation, the diversity orders for the two scenarios are constant, whose values are the same with ideal conditions. This happens because at high SNRs, the second estimation model can capture the exact CSI. Specially, the optimal relay location is obtained by minimize the asymptotic OP. For EC, the *high-SNR slope* and *high-SNR power offset* are zero and infinity due to the noise and estimation error. In addition, the system energy efficiencies of NOMA-based relaying network for the two scenarios were discussed in delay-limited transmission mode.

APPENDIX A: PROOF OF THEOREM 2

Based on the fact that the D_n needs to decode all of the users, whose the channel conditions are worse than its own, and using (16) and (26), the OP of D_n in (25) can be rewritten as

$$P_{out}^n = \underbrace{[1 - \Pr(\tilde{\rho}_{sd_n} > \theta_n^*)]}_{J_1} \quad (A.1)$$
$$\times \underbrace{\left[1 - \Pr\left(\rho_{rd_n} > \psi_n^*, \rho_{sr} > \frac{\psi_n^*(\phi_{2,n}c_2\gamma\rho_{rd_n} + \phi_{3,n})}{\phi_{1,n}c_1\gamma(\rho_{rd_n} - \psi_n^*)}\right)\right]}_{J_2},$$

where $\theta_n^* = \max_{1<j<n} \theta_j$, and $\psi_n^* = \max_{1<j<n} \psi_j$.

Using the PDF of $\tilde{\rho}_{sd_n}$ in (5), J_1 can be obtained as

$$J_1 = F_{\tilde{\rho}_{sd_n}}(\theta_n^*) \quad (A.2)$$
$$= \Xi \sum_{k=0}^{N-n} \binom{N-n}{k} \frac{(-1)^k}{n+k} \left(1 - \sum_{m_1=0}^{\mu_{sd_n}-1} \frac{e^{-\left(\frac{\theta_n^*}{\beta_{sd_n}}\right)^{\frac{\alpha_{sd_n}}{2}}}}{m_1!} \left(\frac{\theta_n^*}{\beta_{sd_n}}\right)^{\frac{\alpha_{sd_n}m_1}{2}}\right)^{n+k}.$$

Next, J_2 can be transformed into

$$J_2 = 1 - \Pr\left(\frac{\rho_{sr}\rho_{rd_n}c_1c_2\gamma^2 \frac{\phi_{1,n}\phi_{2,n}}{\phi_{3,n}^2}}{\frac{\rho_{sr}c_1\gamma\phi_{1,n}}{\phi_{3,n}} + \frac{\rho_{rd_n}c_2\gamma\phi_{2,n}}{\phi_{3,n}} + 1} > \frac{\psi_n^*c_2\gamma\phi_{2,n}}{\phi_{3,n}}\right). \quad (A.3)$$

It is difficult to obtain the exact results, but we can use the inequality $xy/(x+y+1) \le \min(x,y)$ to approximate it as

$$J_2 = 1 - \Pr(\min(\rho_{sr}c_1\phi_{1,n}, \rho_{rd_n}c_2\phi_{2,n}) \ge \psi_n^*c_2\phi_{2,n})$$
$$\quad (A.4)$$
$$= F_{\rho_{sr}}\left(\frac{c_2\psi_n^*\phi_{2,n}}{c_1\phi_{1,n}}\right) + F_{\rho_{rd_n}}(\psi_n^*) - F_{\rho_{sr}}\left(\frac{c_2\psi_n^*\phi_{2,n}}{c_1\phi_{1,n}}\right)F_{\rho_{rd_n}}(\psi_n^*).$$

By using (3), J_2 can be expressed as

$$J_2 = 1 - \sum_{m_2=0}^{\mu_{sr}-1} \sum_{m_3=0}^{\mu_{rd_n}-1} \frac{e^{-\left(\left(\frac{\tau}{\beta_{sr}}\right)^{\frac{\alpha_{sr}}{2}} + \left(\frac{\psi_n^*}{\beta_{rd_n}}\right)^{\frac{\alpha_{rd_n}}{2}}\right)}}{m_2!m_3!} \left(\frac{\tau}{\beta_{sr}}\right)^{\frac{\alpha_{sr}m_2}{2}} \left(\frac{\psi_n^*}{\beta_{rd_n}}\right)^{\frac{\alpha_{rd_n}m_3}{2}}.$$
$$\quad (A.5)$$

where $\tau = \frac{c_2\psi_n^*\phi_{2,n}}{c_1\phi_{1,n}}$.

Substituting (A.2) and (A.5) into (A.1), the proof is completed. For ideal conditions, the OP expression can be obtained by setting $\kappa_i = \sigma_{e_i}^2 = 0$ in Theorem 1.

APPENDIX B: PROOF OF THEOREM 3

For $\alpha - \mu$ fading channels, we can obtain

$$\mathbb{E}\{\tilde{\rho}_{sd_n}\} = \Xi \sum_{k=0}^{n-1} \binom{n-1}{k} \frac{(-1)^k \beta_{sd_n} \Gamma\left(\mu_{sd_n} + \frac{2}{\alpha_{sd_n}}\right)}{\Gamma(\mu_{sd_n})(N-n+k+1)^{\left(\mu_{sd_n} + \frac{2}{\alpha_{sd_n}}\right)}}.$$
$$\quad (B.1)$$

Using the approximation [42]

$$\mathbb{E}\left\{\log_2\left(1 + \frac{x}{y}\right)\right\} \approx \log_2\left(1 + \frac{\mathbb{E}\{x\}}{\mathbb{E}\{y\}}\right). \quad (B.2)$$

and (B.1), (34) can be converted to (35). When $\kappa_i = \sigma_{e_i} = 0$, (35) can be reduce to (36).

$$C^{\text{sum}} = \frac{1}{4} \sum_{n=1}^{N} \left(\log_2 \left(1 + \max \left(\frac{a_n \gamma \mathbb{E}\{\tilde{\rho}_{sd_n}\}}{\gamma \Theta'_n \mathbb{E}\{\tilde{\rho}_{sd_n}\} + \varpi_{sd_n}}, \frac{a_n \gamma^2 \mathbb{E}\{\rho_{sr}\} \mathbb{E}\{\rho_{rd_n}\}}{\gamma^2 \Theta''_n \mathbb{E}\{\rho_{sr}\} \mathbb{E}\{\rho_{rd_n}\} + \phi_{1,n} \gamma \mathbb{E}\{\rho_{sr}\} + \phi_{2,n} \gamma \mathbb{E}\{\rho_{rd_n}\} + \phi_{3,n}} \right) \right) \right.$$
$$\left. + \log_2 \left(1 + \frac{a_n \gamma \mathbb{E}\{\tilde{\rho}_{sd_n}\}}{\gamma \Theta'_n \mathbb{E}\{\tilde{\rho}_{sd_n}\} + \varpi_{sd_n}} \right) \right). \quad \text{(C.1)}$$

APPENDIX C: PROOF OF THEOREM 4

By applying the equality (B.2), (45) can be converted to (C.1), shown at the bottom of the next page.

For $\alpha - \mu$ fading channels, we can obtain

$$\mathbb{E}\{\rho_I\} = \frac{\beta_I \Gamma\left(\mu_I + \frac{2}{\alpha_I}\right)}{\Gamma(\mu_I)}, I = sr, rd_n, \quad \text{(C.2)}$$

By plugging (C.2) and (B.1) into (C.1), we can obtain (46). When $\kappa_i = \sigma_{e_i} = 0$, (46) can be reduce to (47). In the special case of ideal conditions, the closed-form expression for the EC of users can be obtained by setting $\kappa_i = \sigma_{e_i}^2 = 0$ in **Theorem 4**.

REFERENCES

[1] X. Li, J. Li, Y. Liu, Z. Ding, and A. Nallanathan, "Outage performance of cooperative NOMA networks with hardware impairments," in *IEEE Global Communications Conference (GLOBECOM)*, Dec. 2018, pp. 1–6.

[2] Q. C. Li, H. Niu, A. T. Papathanassiou, and G. Wu, "5G network capacity: Key elements and technologies," *IEEE Veh. Technol. Mag.*, vol. 9, no. 1, pp. 71–78, Mar. 2014.

[3] L. Dai, B. Wang, Y. Yuan, S. Han, C. l. I, and Z. Wang, "Non-orthogonal multiple access for 5G: solutions, challenges, opportunities, and future research trends," *IEEE Commun. Mag.*, vol. 53, no. 9, pp. 74–81, Sep. 2015.

[4] L. Yu, P. Fan, X. Lei, and P. T. Mathiopoulos, "BER analysis of SCMA systems with codebooks based on star-QAM signaling constellations," *IEEE Commun. Lett.*, vol. 21, no. 9, pp. 1925–1928, Sep. 2017.

[5] S. M. R. Islam, N. Avazov, O. A. Dobre, and K. Kwak, "Power-domain non-orthogonal multiple access (NOMA) in 5G systems: Potentials and challenges," *IEEE Commun. Surveys Tuts.*, vol. 19, no. 2, pp. 721–742, 2nd Quart. 2017.

[6] X. Li, J. Li, and L. Li, "Performance analysis of impaired SWIPT NOMA relaying networks over imperfect Weibull channels," *IEEE Syst. J.*, pp. 1–4, 2019.

[7] Z. Ding, Z. Yang, P. Fan, and H. V. Poor, "On the performance of non-orthogonal multiple access in 5G systems with randomly deployed users," *IEEE Signal Process. Lett.*, vol. 21, no. 12, pp. 1501–1505, Dec. 2014.

[8] N. Zhang, J. Wang, G. Kang, and Y. Liu, "Uplink nonorthogonal multiple access in 5G systems," *IEEE Commun. Lett.*, vol. 20, no. 3, pp. 458–461, Mar. 2016.

[9] Y. Liu, Z. Qin, M. Elkashlan, Y. Gao, and L. Hanzo, "Enhancing the physical layer security of non-orthogonal multiple access in large-scale networks," *IEEE Trans. Wireless Commun.*, vol. 16, no. 3, pp. 1656–1672, Mar. 2017.

[10] Y. Liu, Z. Ding, M. Elkashlan, and H. V. Poor, "Cooperative non-orthogonal multiple access with simultaneous wireless information and power transfer," *IEEE J. Sel. Areas Commun.*, vol. 34, no. 4, pp. 938–953, Apr. 2016.

[11] 3rd Generation Partnership Projet (3GPP), "Study on downlink multiuser superposition transmation for LTE, TSG RAN meeting 67," *Tech. Rep. RP-150496*, Mar. 2015.

[12] 3rd Generation Partnership Projet, "Study on Non-Orthogonal Multiple Access (NOMA) for NR, TSG RAN," *3GPP Tech. Rep. 38.812*, Feb. 2018.

[13] Y. Liu, Z. Qin, M. Elkashlan, A. Nallanathan, and J. A. McCann, "Non-orthogonal multiple access in large-scale heterogeneous networks," *IEEE J. Sel. Areas Commun.*, vol. 35, no. 12, pp. 2667–2680, Dec. 2017.

[14] T. Schenk, *RF Imperfections in High-Rate Wireless Systems: Impact and Digital Compensation*. Berlin, NY, Germany: Springer-Verlag, 2008.

[15] E. Björnson, J. Hoydis, M. Kountouris, and M. Debbah, "Massive MIMO systems with non-ideal hardware: Energy efficiency, estimation, and capacity limits," *IEEE Trans. Inf. Theory*, vol. 60, no. 11, pp. 7112–7139, Nov. 2014.

[16] C. Studer, M. Wenk, and A. Burg, "MIMO transmission with residual transmit-RF impairments," in *IEEE Proc. ITG Work. Smart Ant. (WSA)*, Feb. 2010, pp. 189–196.

[17] E. Björnson, P. Zetterberg, M. Bengtsson, and B. Ottersten, "Capacity limits and multiplexing gains of MIMO channels with transceiver impairments," *IEEE Commun. Lett.*, vol. 17, no. 1, pp. 91–94, Jan. 2013.

[18] X. Zhang, M. Matthaiou, M. Coldrey, and E. Bjrnson, "Impact of residual transmit RF impairments on training-based MIMO systems," *IEEE Trans. Commun.*, vol. 63, no. 8, pp. 2899–2911, Aug. 2015.

[19] T. T. Duy, T. Q. Duong, D. B. da Costa, V. N. Q. Bao, and M. Elkashlan, "Proactive relay selection with joint impact of hardware impairment and co-channel interference," *IEEE Trans. Commun.*, vol. 63, no. 5, pp. 1594–1606, May 2015.

[20] X. Yue, Y. Liu, S. Kang, A. Nallanathan, and Z. Ding, "Exploiting full/half-duplex user relaying in NOMA systems," *IEEE Trans. Commun.*, vol. 66, no. 2, pp. 560–575, Sep. 2017.

[21] R. Jiao, L. Dai, J. Zhang, R. MacKenzie, and M. Hao, "On the performance of NOMA-based cooperative relaying systems over Rician fading channels," *IEEE Trans. Veh. Technol.*, vol. 66, no. 12, pp. 11 409–11 413, Dec. 2017.

[22] J. Men, J. Ge, and C. Zhang, "Performance analysis of nonorthogonal multiple access for relaying networks over Nakagami-m fading channels," *IEEE Trans. Veh. Technol.*, vol. 66, no. 2, pp. 1200–1208, Feb. 2017.

[23] E. Björnson, M. Matthaiou, and M. Debbah, "A new look at dual-hop relaying: Performance limits with hardware impairments," *IEEE Trans. Commun.*, vol. 61, no. 11, pp. 4512–4525, Nov. 2013.

[24] M. Matthaiou, A. Papadogiannis, E. Bjornson, and M. Debbah, "Two-way relaying under the presence of relay transceiver hardware impairments," *IEEE Commun. Lett.*, vol. 17, no. 6, pp. 1136–1139, Jun. 2013.

[25] N. T. Do, D. B. da Costa, and B. An, "Performance analysis of multirelay RF energy harvesting cooperative networks with hardware impairments," *IET Commun.*, vol. 10, no. 18, pp. 2551–2558, Dec. 2016.

[26] F. Ding and H. Wang and S. Zhang and M. Dai, "Impact of residual hardware impairments on non-orthogonal multiple access based amplify-and-forward relaying networks," *IEEE Access*, vol. 6, pp. 15 117–15 131, 2018.

[27] D. Wan and M. Wen and F. Ji and Y. Liu and Y. Huang, "Cooperative NOMA systems with partial channel state information over Nakagami-m fading channels," *IEEE Trans. Commun.*, vol. 66, no. 3, pp. 947–958, Mar. 2018.

[28] Z. Yang, Z. Ding, P. Fan, and G. K. Karagiannidis, "On the performance of non-orthogonal multiple access systems with partial channel information," *IEEE Trans. Commun.*, vol. 64, no. 2, pp. 654–667, Feb. 2016.

[29] N. I. Miridakis and T. A. Tsiftsis, "On the joint impact of hardware impairments and imperfect CSI on successive decoding," *IEEE Trans. Veh. Technol.*, vol. 66, no. 6, pp. 4810–4822, Jun. 2017.

[30] X. Chen, R. Jia, and D. W. K. Ng, "On the design of massive non-orthogonal multiple access with imperfect successive interference cancellation," *IEEE Trans. Commun.*, vol. 67, no. 3, pp. 2539–2551, Mar. 2019.

[31] M. D. Yacoub, "The α - μ distribution: A physical fading model for the stacy distribution," *IEEE Trans. Veh. Techn.*, vol. 56, no. 1, pp. 27–34, Jan. 2007.

[32] X. Yue, Y. Liu, S. Kang, and A. Nallanathan, "Performance analysis of NOMA with fixed gain relaying over Nakagami-m fading channels," *IEEE Access*, vol. 5, 2017.

[33] L. Wang, Y. Cai, and W. Yang, "On the finite-SNR DMT of two-way

AF relaying with imperfect CSI," *IEEE Wireless Commun. Lett.*, vol. 1, no. 3, pp. 161–164, Jun. 2012.

[34] W. M. Gifford, M. Z. Win, and M. Chiani, "Diversity with practical channel estimation," *IEEE Trans. Wireless Commun.*, vol. 4, no. 4, pp. 1935–1947, Jul. 2005.

[35] O. S. Badarneh and R. Mesleh, "A comprehensive framework for quadrature spatial modulation in generalized fading scenarios," *IEEE Trans. Commun.*, vol. 64, no. 7, pp. 2961–2970, Nov. 2006.

[36] H. A. David and H. N. Nagaraja, *Order Statistics*, 3rd ed.   New York, NY, USA: Wiley, 2003.

[37] S. S. Ikki and S. Aissa, "Two-way amplify-and-forward relaying with Gaussian imperfect channel estimations," *IEEE Commun. Lett.*, vol. 16, no. 7, pp. 956–959, Jul. 2012.

[38] S. Stefania, B. Matthew, and T. Issam, *LTE-the UMTS long term evolution: from theory to practice*, 2nd ed.   New York, NY, USA: Wiley & Sons, 2011.

[39] E. Biglieri, R. Calderbank, A. Constantinides, A. Goldsmith, A. Paulraj, and H. V. Poor, *MIMO wireless communications*.   Cambridge university press, 2007.

[40] M. Tatar Mamaghani and A. Kuhestani and K. Wong, "Secure two-way transmission via wireless-powered untrusted relay and external jammer," *IEEE Trans. Veh. Technol*, pp. 1–1, 2018.

[41] X. Li and J. Li and L. Li and L. Du and J. Jin and D. Zhang, "Performance analysis of cooperative small cell systems under correlated Rician/Gamma fading channels," *IET Signal Process.*, vol. 12, no. 1, pp. 64–73, 2018.

[42] Q. Zhang and S. Jin and K. Wong and H. Zhu and M. Matthaiou, "Power scaling of uplink massive MIMO systems with arbitrary-rank channel means," *IEEE J. Sel. Topics Signal Process.*, vol. 8, no. 5, pp. 966–981, Oct. 2014.